

**Ceramic, Composite and  
Optical Materials Center**

Patrick Kwon  
Mechanical Engineering  
Michigan State University  
East Lansing, Michigan  
[pkwon@egr.msu.edu](mailto:pkwon@egr.msu.edu)  
(517) 355-0173



# Active & Prospective Members

- 1. Boeing, Seattle, WA
- 2. Fraunhofer CCL, East Lansing, MI
- 3, 4. Los Alamos National Lab, NM
- 5. Diamond Innovation/Valenite, Columbus, OH
- 6. ARMY ARDEC
- GM Powertrain
- Pratt & Whitney
- Caterpillar, Peoria, IL
- General Dynamic, St. Petersburg, FL
- Ford Motor Company
- Nexteer (Delphi)
- General Electric



# Current Projects

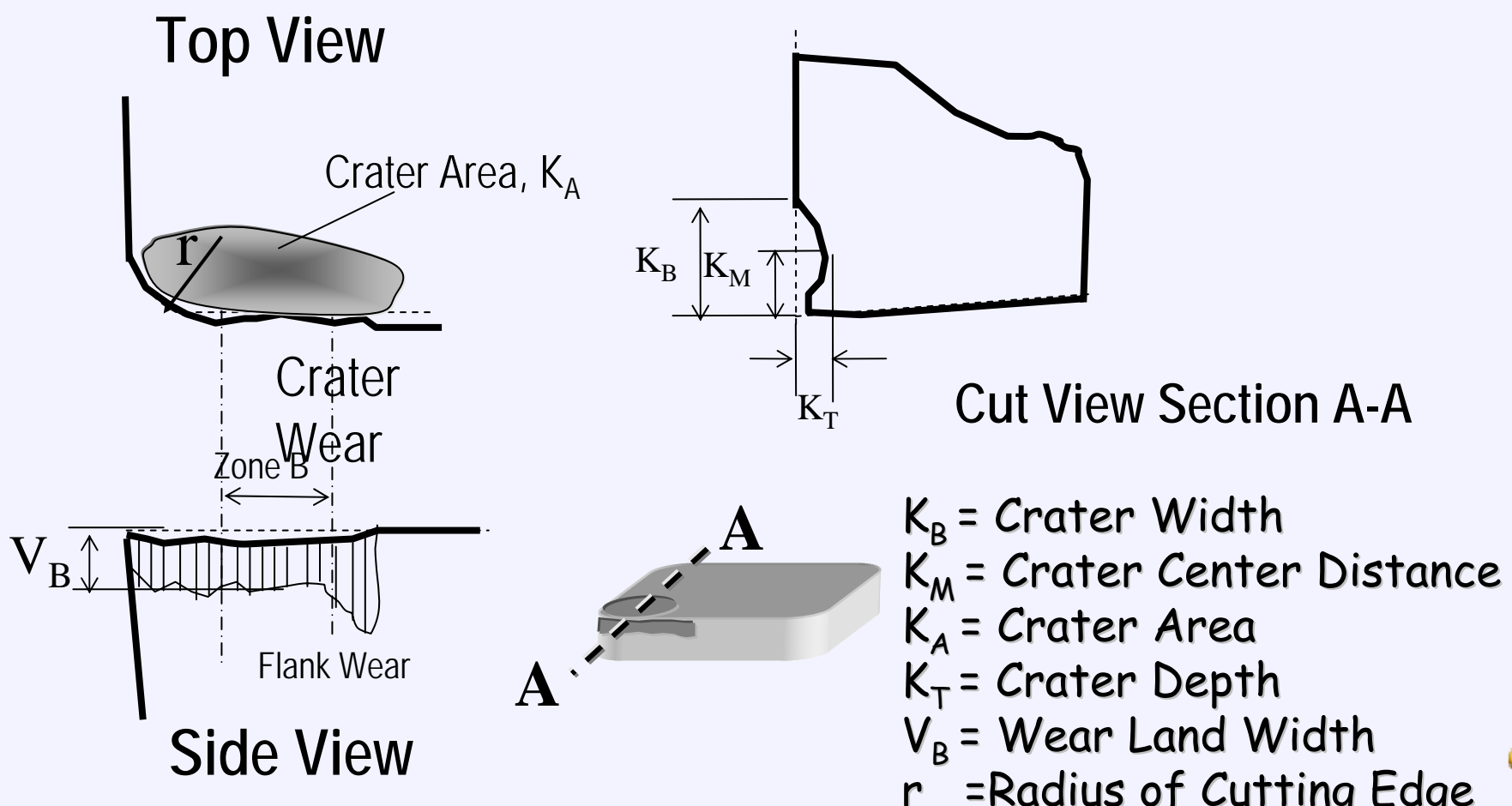
- Drilling of Composite/Metal Stack (Boeing, New Tech Ceramic & Fraunhofer)
  - Carbides, PCD & Coated Carbides
- Soft Machining (LANL & Valenite)
  - Adhesion
- Machining Titanium (ARMY-ARDEC & DI)
  - Tool Wear mechanisms
- Advanced Cutting Tool Systems (LANL-Fraunhofer)
  - Stacking sequence & thickness of Multi-layer Coatings
- MQL with Nanoenhanced-Lubricant (UNIST & XG Science)
- Many other projects are possible with other faculty at MSU.



# Tool Wear Approach

Still, an empirical approach

*Taylor's Model* :  $V^a d^b f^c = \text{constant}$



# Possible Wear Mechanisms

## Mechanical wear

- **Abrasive wear**
  - The sliding and rolling of hard second phase on the work/tool materials interface
- **Delamination Wear**
  - Continual loading leads to subsurface cracks propagation
- **Adhesion (AI)**
  - Welding of asperity junctions

## Thermochemical wear

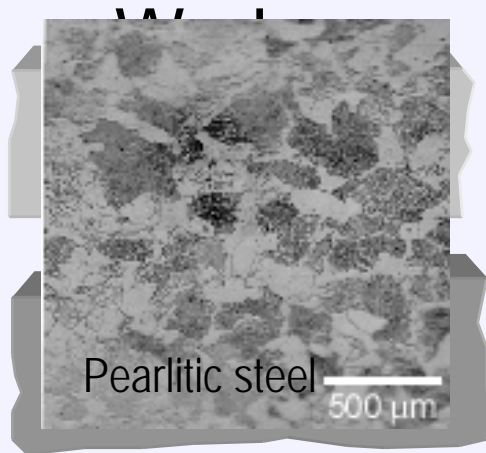
- **Dissolution Wear**
  - Thermally activated mechanisms - Atomic transport across the interface
- **Diffusion wear**
  - The component of tool materials can be diffused into chips
- **Chemical reaction (Ti)**
  - Chemical reaction between tool and work material

- Thermomechanical fatigue

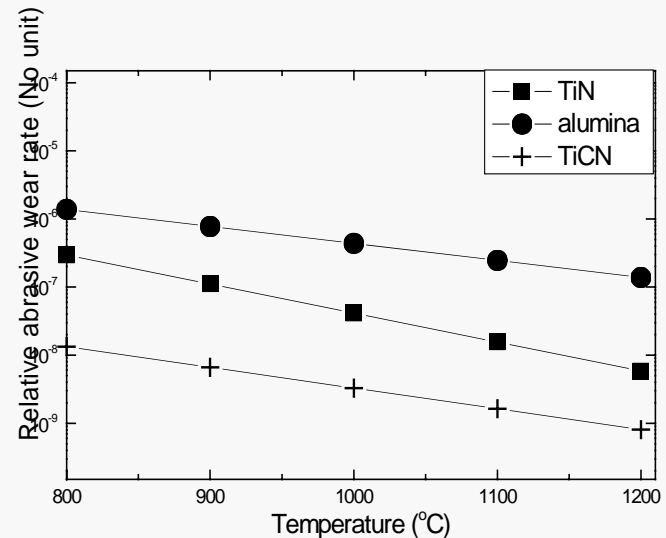
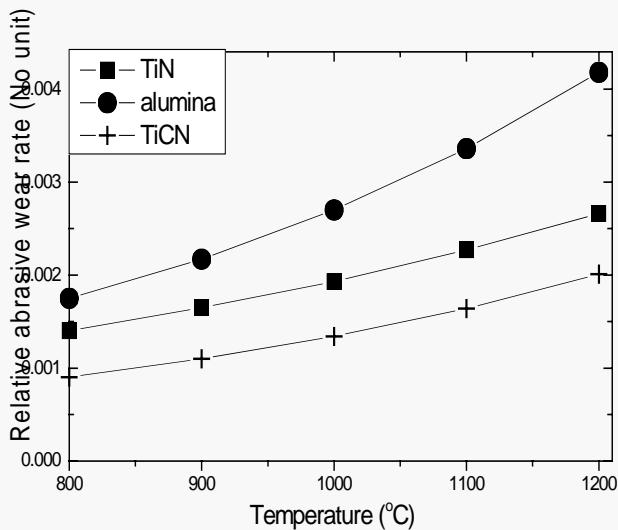
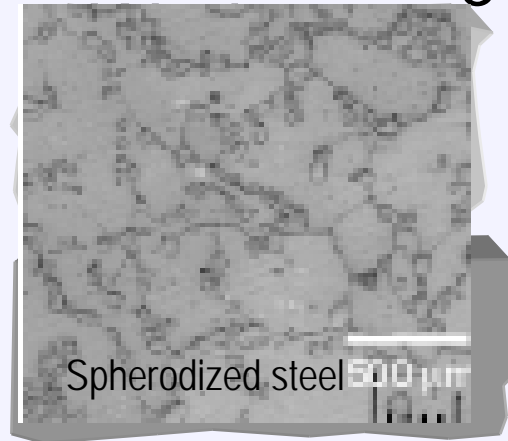


# Abrasive Wear Models

2-body Wear



3-body Wear



# Amount of Abrasives: Compositions of Steels

(All in wt%)

	C	Mn	P	S	Si	Ni	Cr	Mo
1018	0.21	0.70	0.02	0.03	0.21	0.07	0.13	0.02
1045	0.48	0.74	0.01	0.04	0.27	0.05	0.08	0.02
1070	0.68	0.78	0.01	0.02	0.22	0.04	0.17	0.02
1018 (S)	0.16	0.83	0.01	0.03	0.20	0.01	0.08	0.01
1045 (S)	0.48	0.74	0.01	0.04	0.27	0.05	0.08	0.02
1065 (S)	0.64	0.80	0.01	0.01	0.28	0.07	0.15	0.02
1095 (S)	0.89	1.02	0.02	0.03	0.31	0.15	0.32	0.14

- Round Bar stocks: nominally of diameters between 3" and 6" and length about 2-1/2' initially.

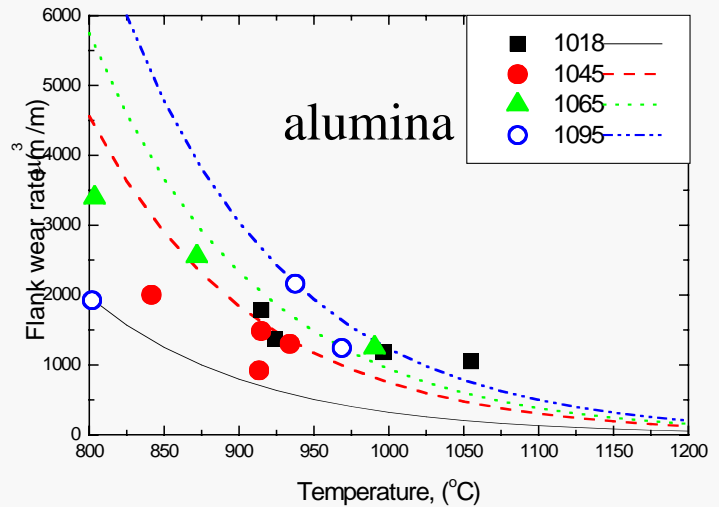
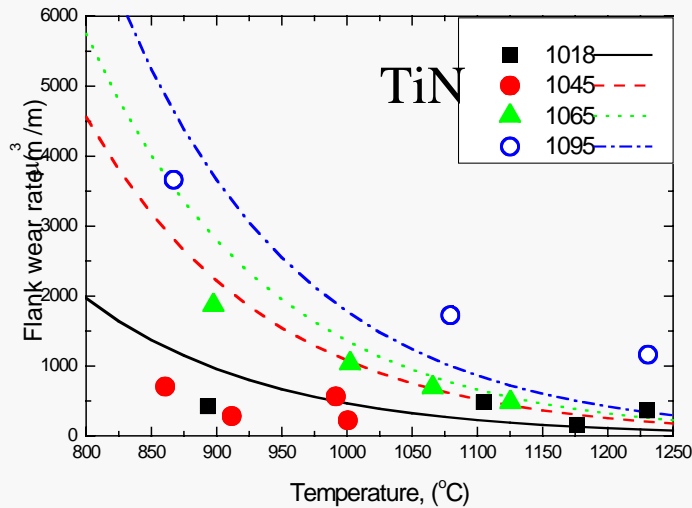
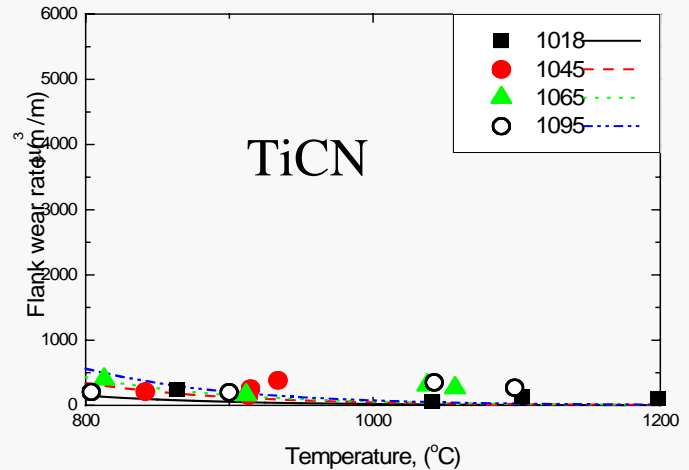


# Flank Wear - Spherodized

Flank Wear Rate

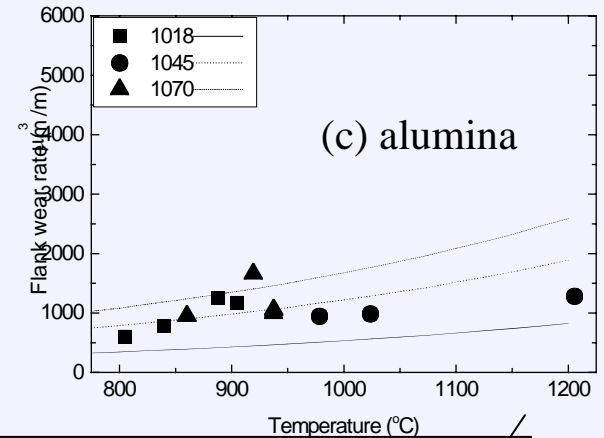
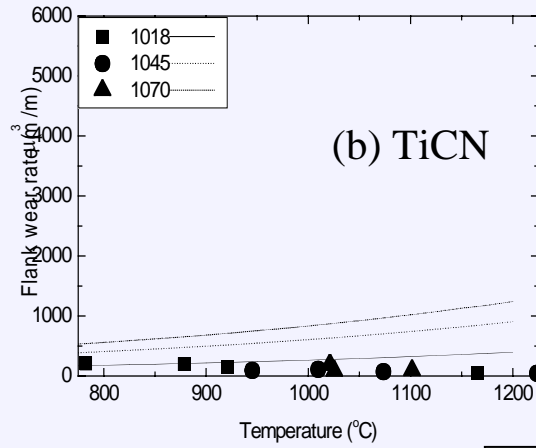
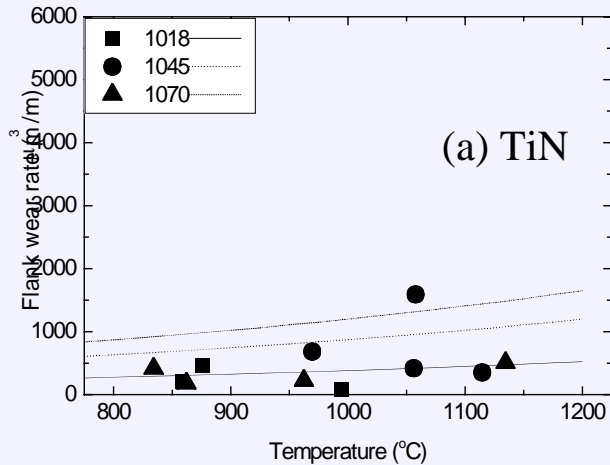
$$= 1.166A(P_a^{(n-1)})/P_t^n$$

Area fraction, A	
steel	A
1018	0.07
1045	0.16
1065	0.21
1095	0.27

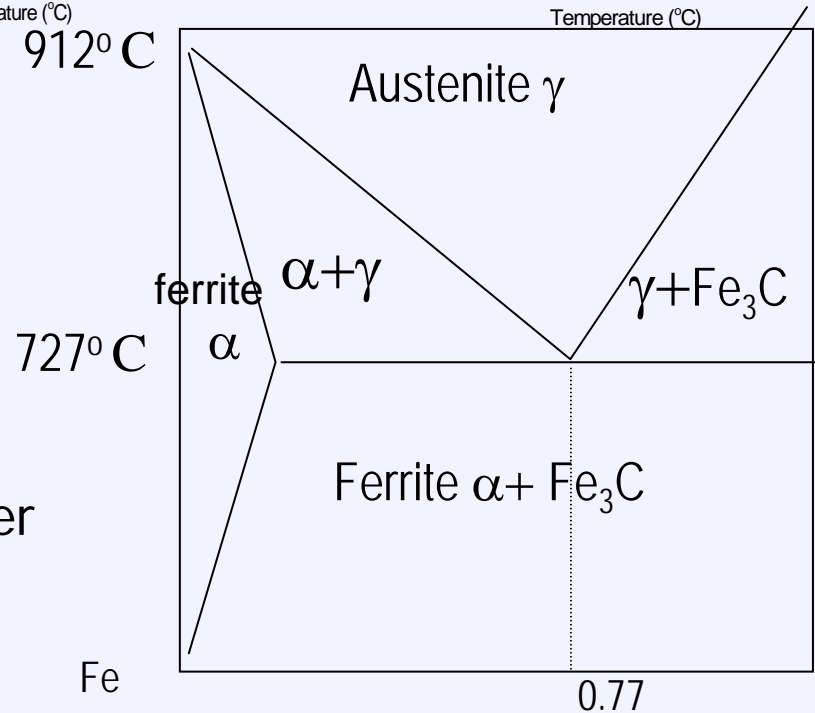




# Flank Wear - Pearlitic



- The Inadequacy of 2-body Abrasive Wear Model
  - TiCN – too low wear
  - No cementite effect - Phase Transformation
  - 4340 & 52100 steels – white layer



# Dissolution Wear Model

The material pair in sliding will dissolve to each other if the free energy of the material pair decreases by the formation of solution.

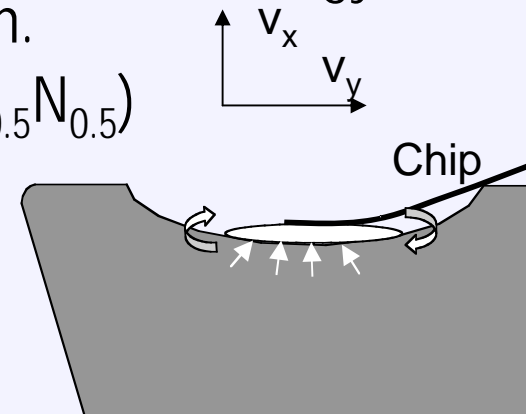
Dissolution wear rate for tertiary coating,  $A_x B_y C_z$  ( $Ti_1 C_{0.5} N_{0.5}$ )  
(Kramer & Suh, 1980; Kramer & Kwon, 1985)

$$BMV^{0.5} C_{A_x B_y C_z}$$

B = the dissolution wear coefficient

M = molar volume of the coating material in  $cm^3/mol$

V = cutting speed (m/min)



Atomic transport across the interface

$$\text{Solubility } C_{A_x B_y C_z} = \exp \left[ \frac{\Delta G_{A_x B_y C_z} - x \Delta G_A^{xs} - y \Delta G_B^{xs} - z \Delta G_C^{xs} - RT(x \ln x + y \ln y + z \ln z)}{(x + y + z)RT} \right]$$

$\Delta G_{A_x B_y C_z}$  = free energy of formation

$\Delta G_i^{xs}$  = excess free energy of i component

R = gas constant

T = temperature (K)



# Dissolution Wear Rate

Tool Materials	Predicted Relative Wear Rate	Estimated Time for 25 $\mu$ m of wear
ZrO <sub>2</sub>	0.0000367	26.053 26 month
Al <sub>2</sub> O <sub>3</sub>	0.00124	27.051 23 days
TiO <sub>2</sub>	0.00313	21 hr
HfN	0.680	60 min
HfC	1.	41 min
TiN	5.92	6.9 min
TiC	12.8	3.2 min
BN	57.0	43 sec
WC	332.	7.4 sec
Diamond	445	5.5 sec

At 1300° C into iron

At 1100° C into Ti



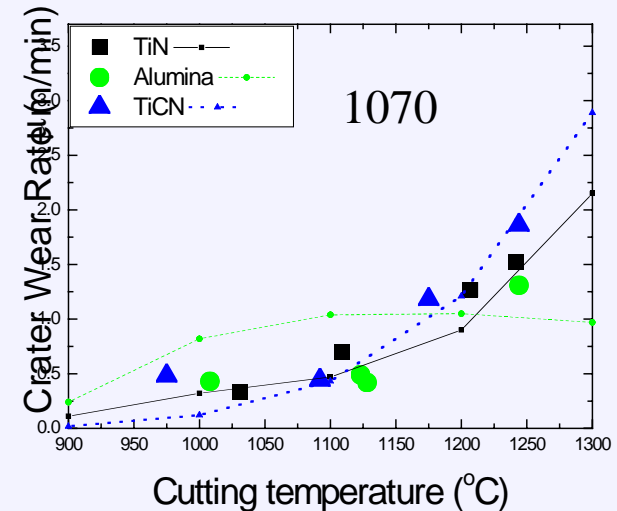
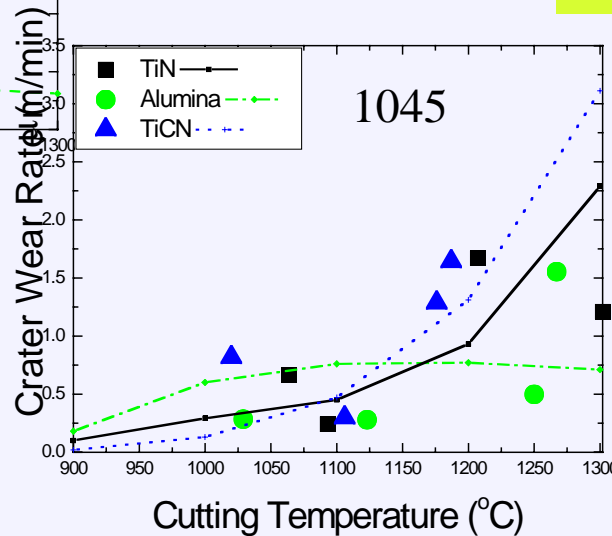
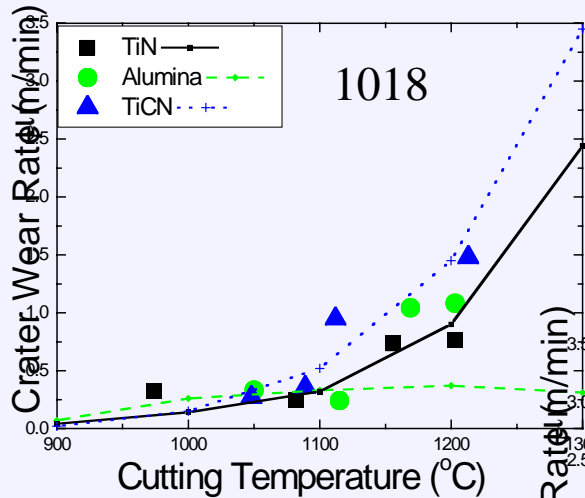
# Crater Wear – Pearlitic

$$\text{Crater Wear Rate} = K_{\text{abs}} AV (P_a^{(n-1)})/P_t^n + K_{\text{dis}} (1-A)MV^{0.5} C_{A_xB_yC_z}$$

3-body Abrasive Wear      Dissolution Wear

Cutting coefficient, $K_{\text{abs}}$	Cutting coefficient, $K_{\text{dis}}$
145	31

Dissolve into Austenite Phase

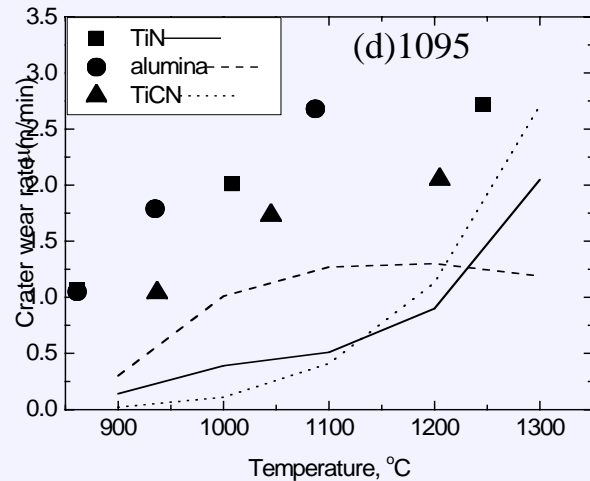
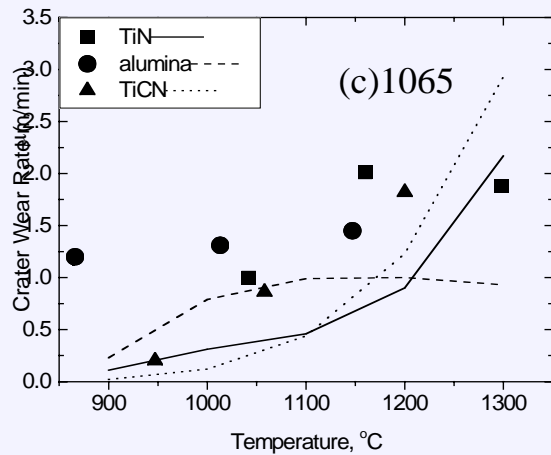
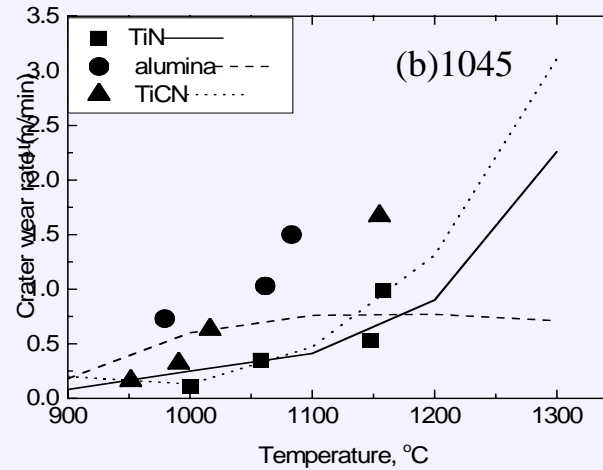
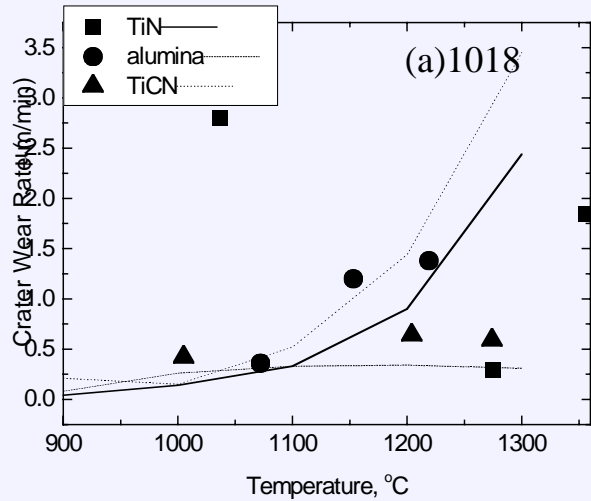


Problem with Alumina



# Crater Wear - Spherodized

Dissolve into ferrite Phase



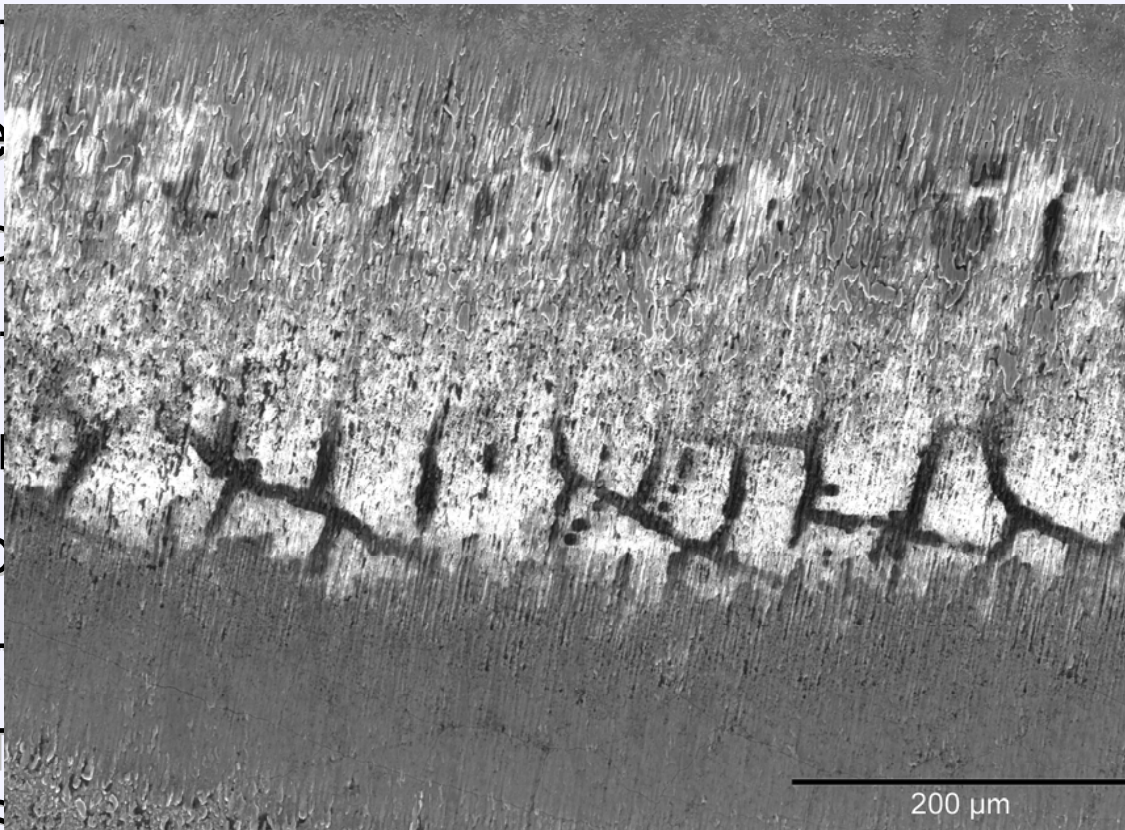
High Vanadium



# Effectiveness of Multi-layer coating (LANL)

- Experiments - Turning AISI 1045 Steels

- Cut
- Fee
- Dep
- Cut
- Wor
- App
- Cut



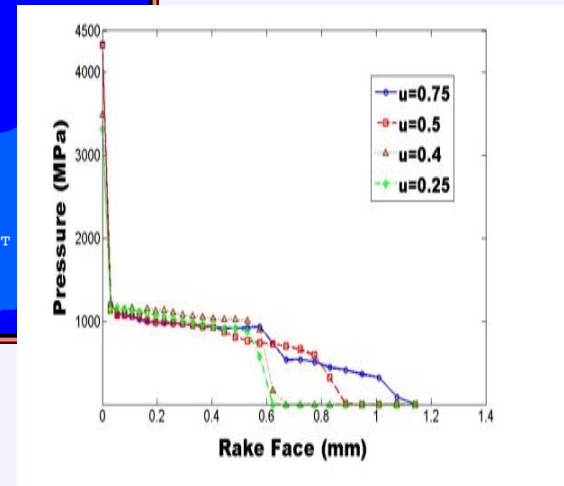
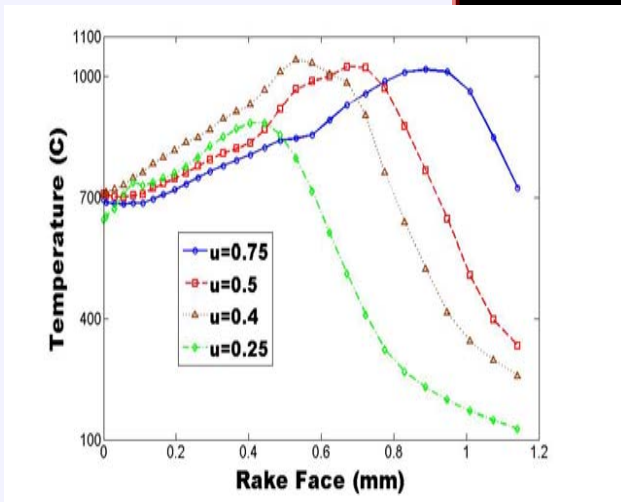
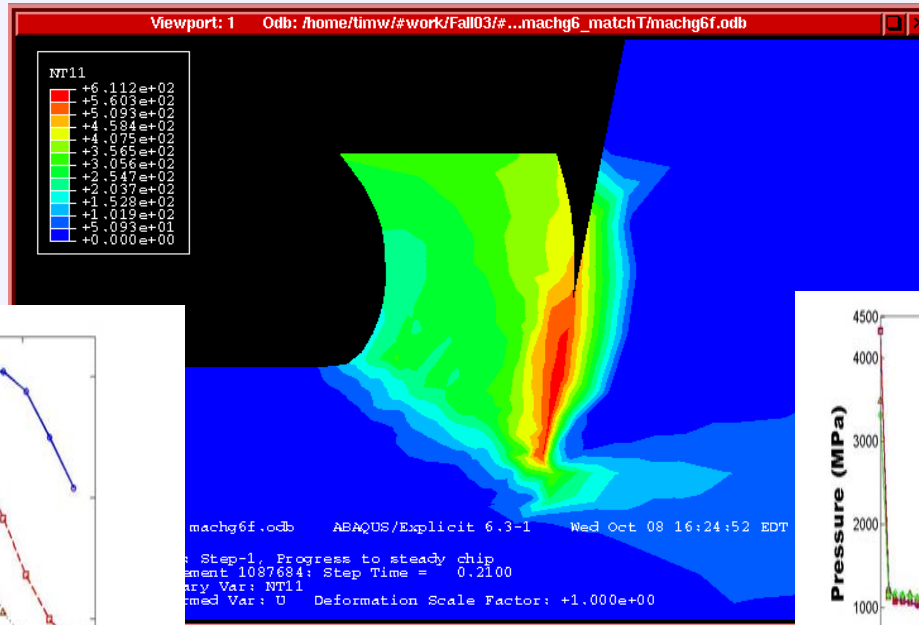
& 480s.

- T
- Substrate



# FE simulation - ABAQUS Modeling

- Arbitrary Lagrangian and Eulerian (ALE) Formulation
  - Tool and Work Material (Johnson-Cook Model for 1045 steels)
- Constitutive & Friction models



Rake Face

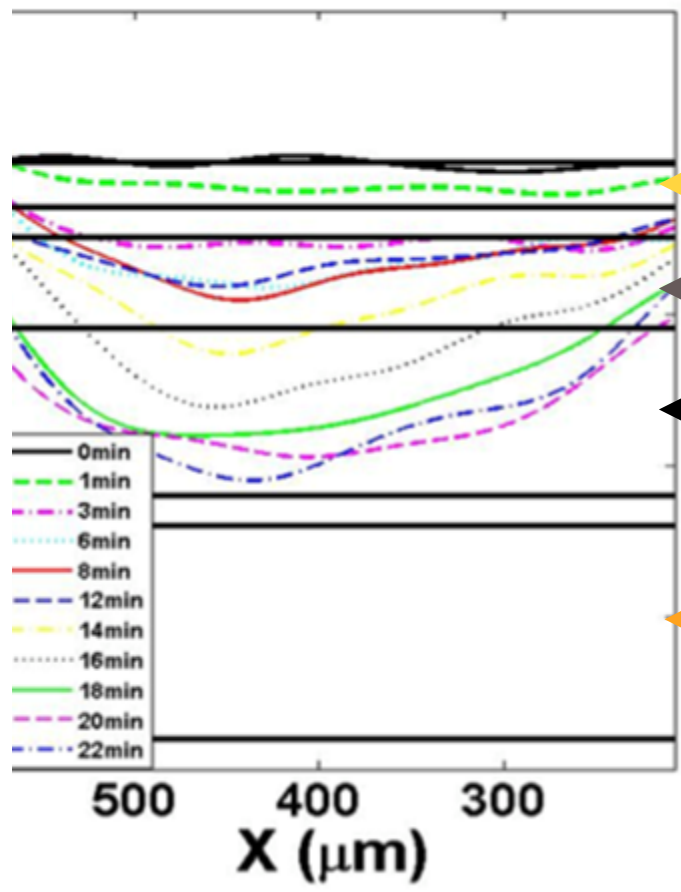
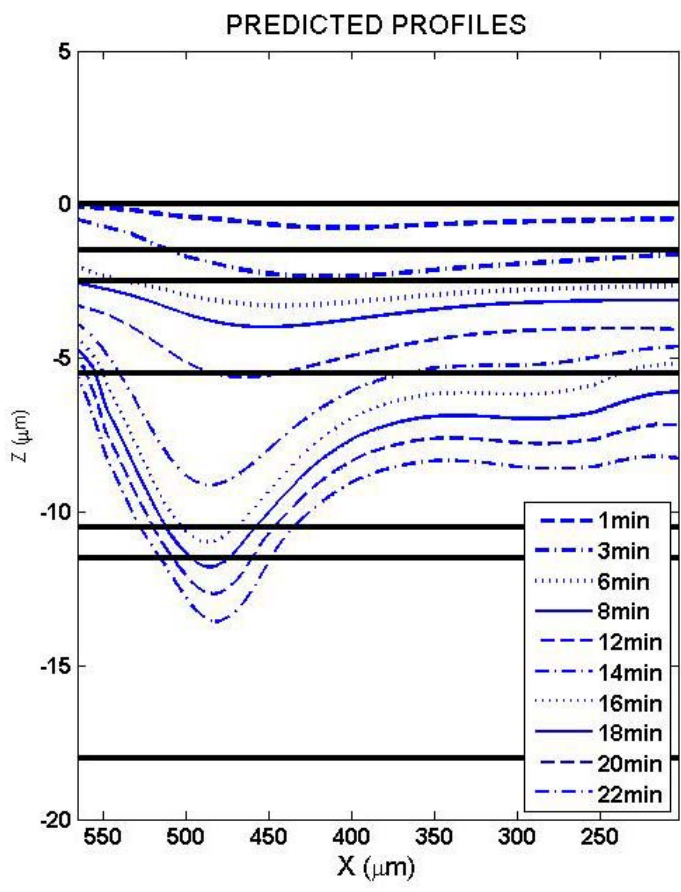
Contact Length



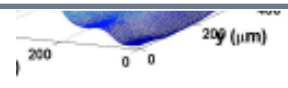
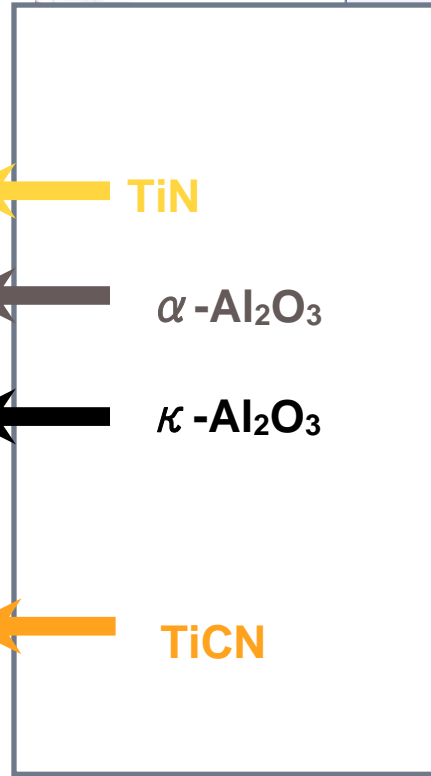
# Crater Wear Summary

Tuning of 1045 steel with multilayer(TiN/Al<sub>2</sub>O<sub>3</sub>/TiCN) coating

## EXPERIMENTAL PROFILES



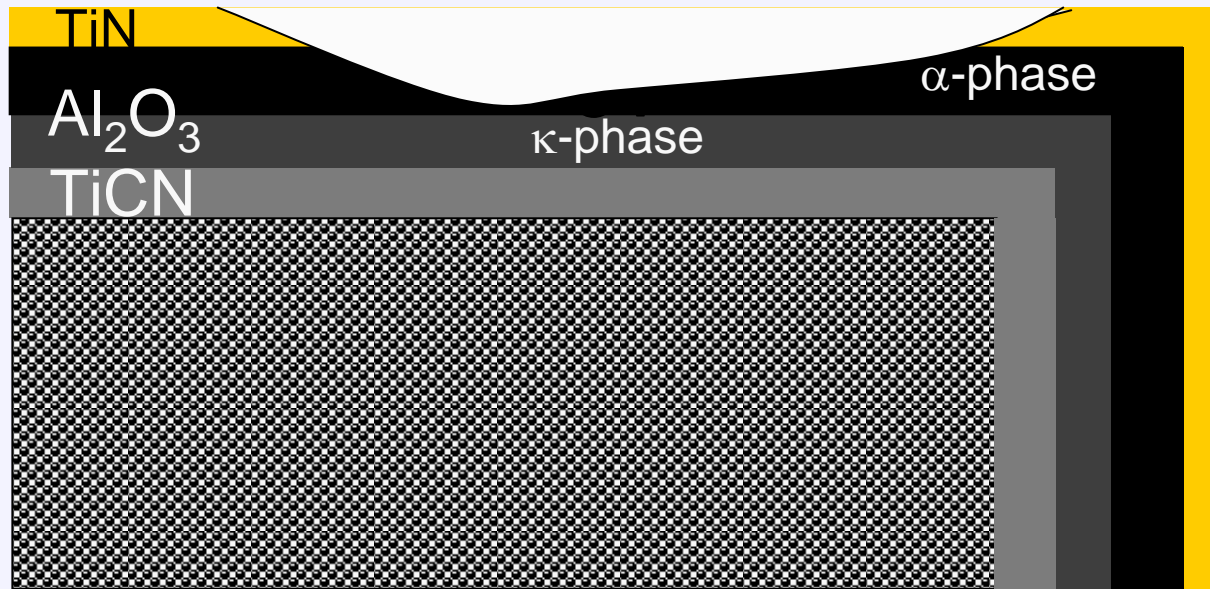
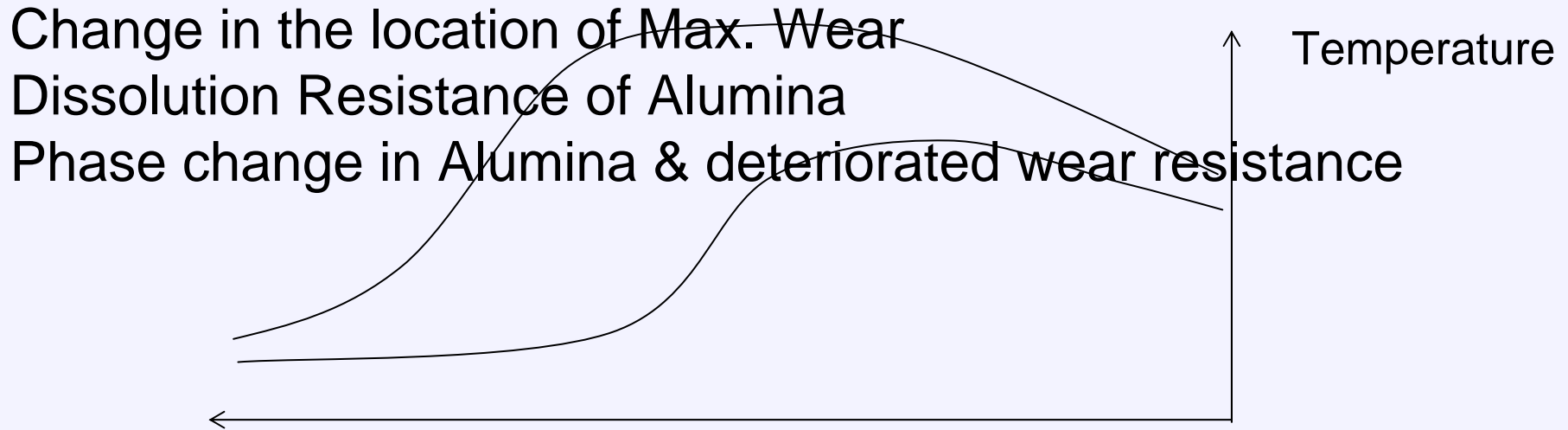
A1 - 3 min



Crater wear evolution



# Interpretation of Results



# New Experimental Setup

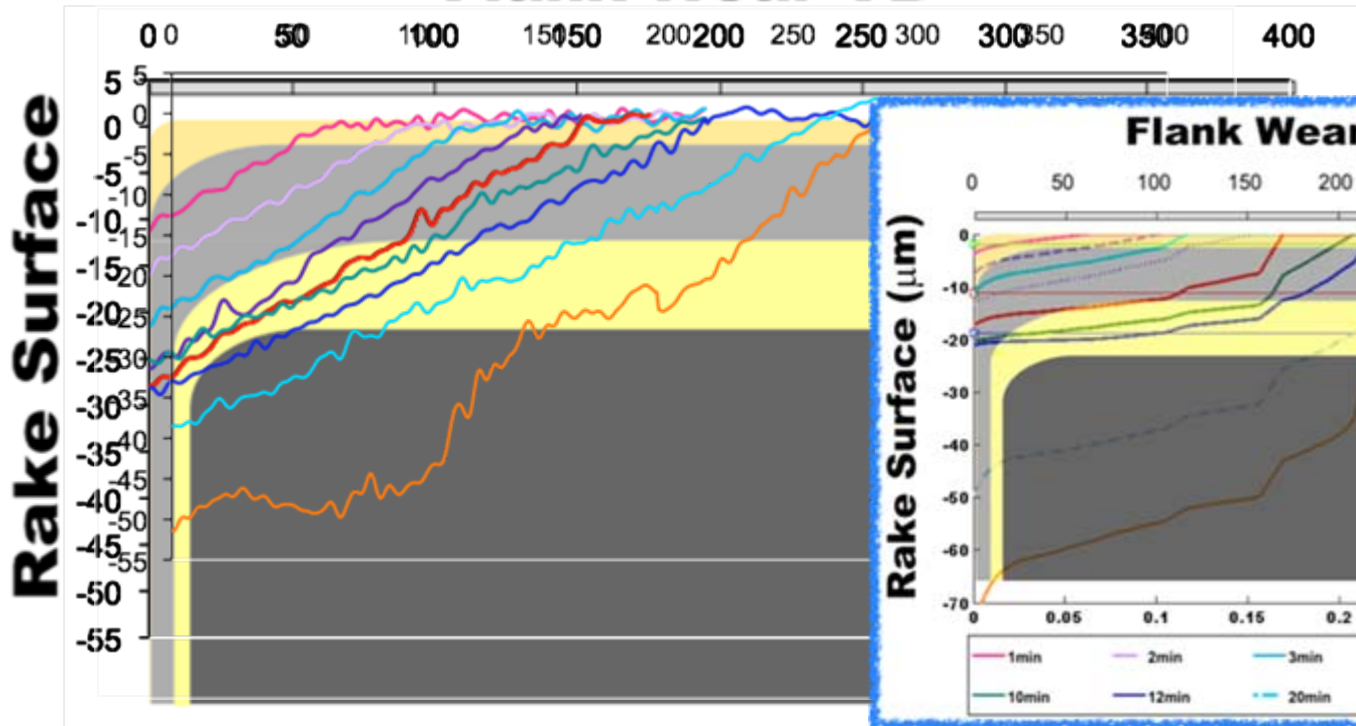
- Turning of 1045 steels till carbide is exposed
- Four coatings on WC-6%Co substrates:
  - Boron Aluminum Magnesium ( $\text{AlMgB}_{14}$ ) and  $\text{TiB}_2$  alloy (BAM) \*
  - $\text{AlTiN}+\text{Si}_3\text{N}_4$  binder (C7 nano-composite) provided by UNIMERCO Inc., Saline, MI.
  - $\text{AlTiN}$  \*
  - $\text{TiN}$  \*
- Sandvik Flat Carbide Inserts (SCMW 432)
- Determining **Friction** for each coating

\* Coating provided by Fraunhofer, Inc., Michigan State University

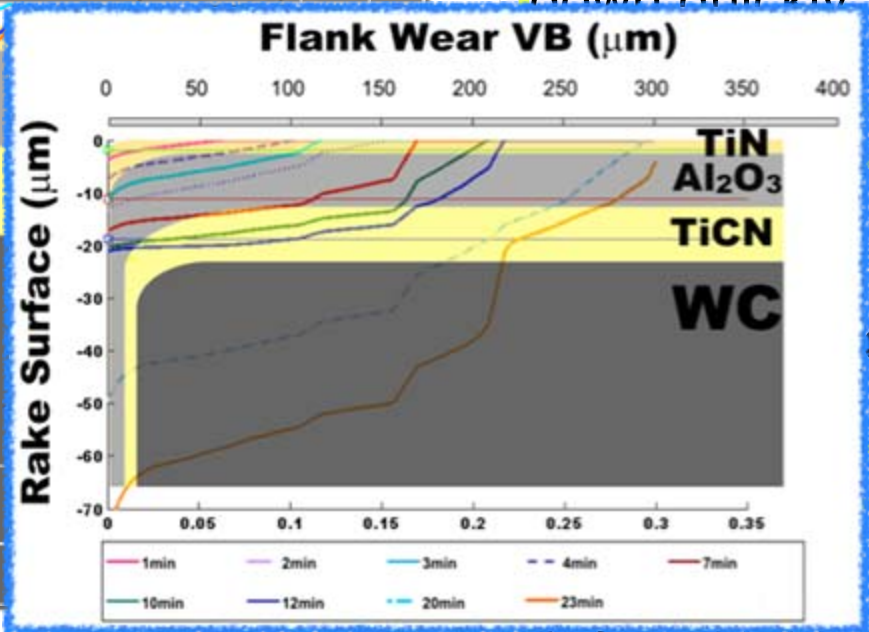


# Flank Wear Evolution

**Flank Wear VB**



TiN + Al<sub>2</sub>O<sub>3</sub> Coatings wear down quickly



ce

BATCH	<u>TiN</u>	Al <sub>2</sub> O <sub>3</sub>	<u>TiCN</u>
Ave. Coating Thickness	1.94μm	9.16μm	7.58μm

worn down at 20-23 min

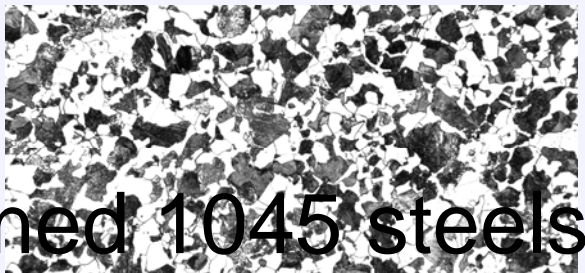
Hardness: Al<sub>2</sub>O<sub>3</sub> < TiN < TiCN



# 1045 Normalized & Refined

Normalized & Grain Refined AISI1045

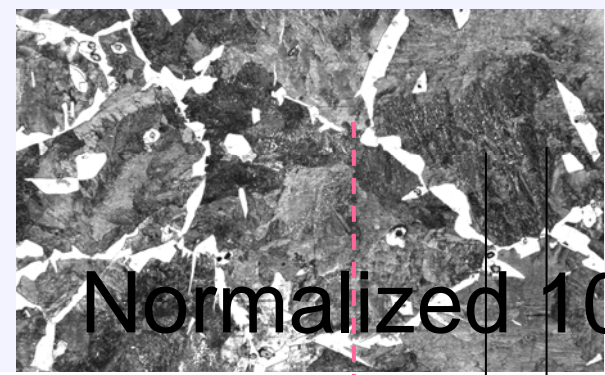
168 VHN



Refined 1045 steels 200x

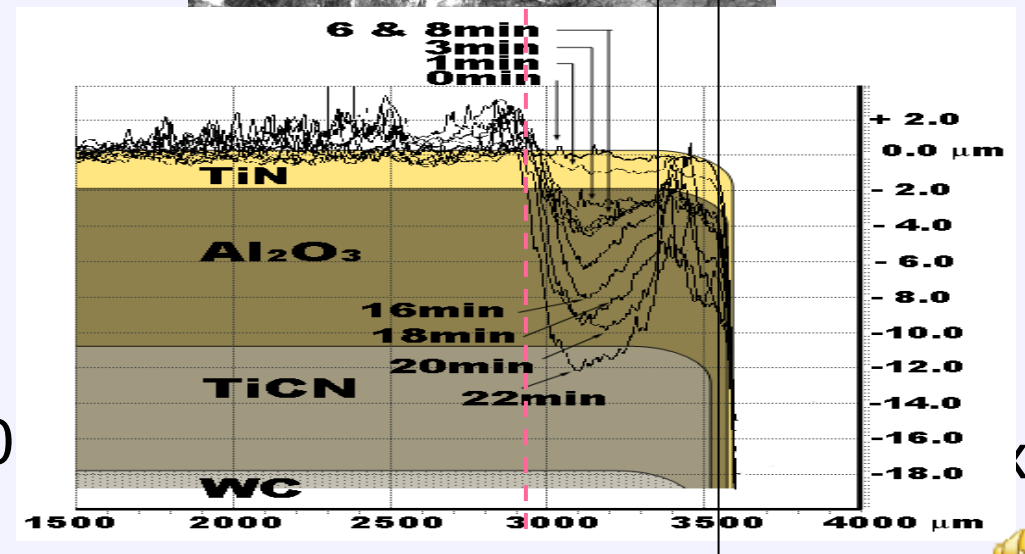
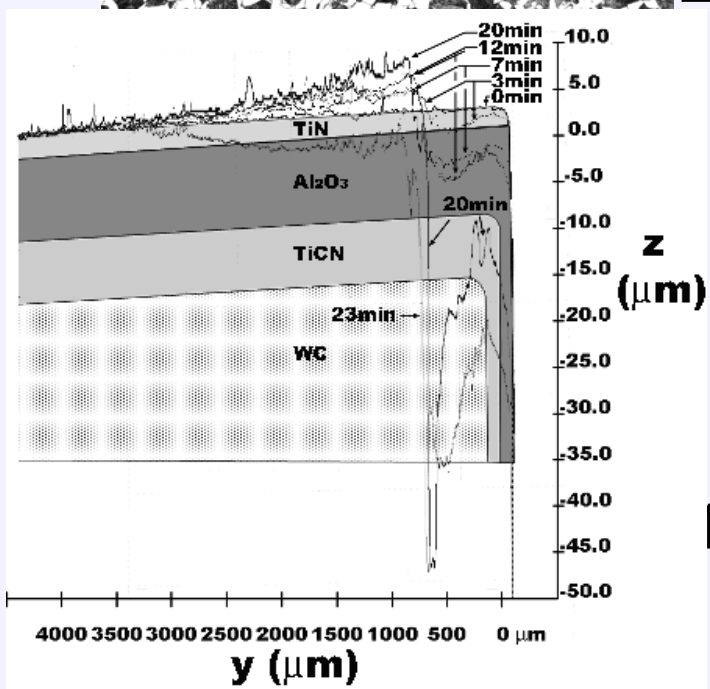
Normalized AISI1045

211 VHN



Normalized 1045

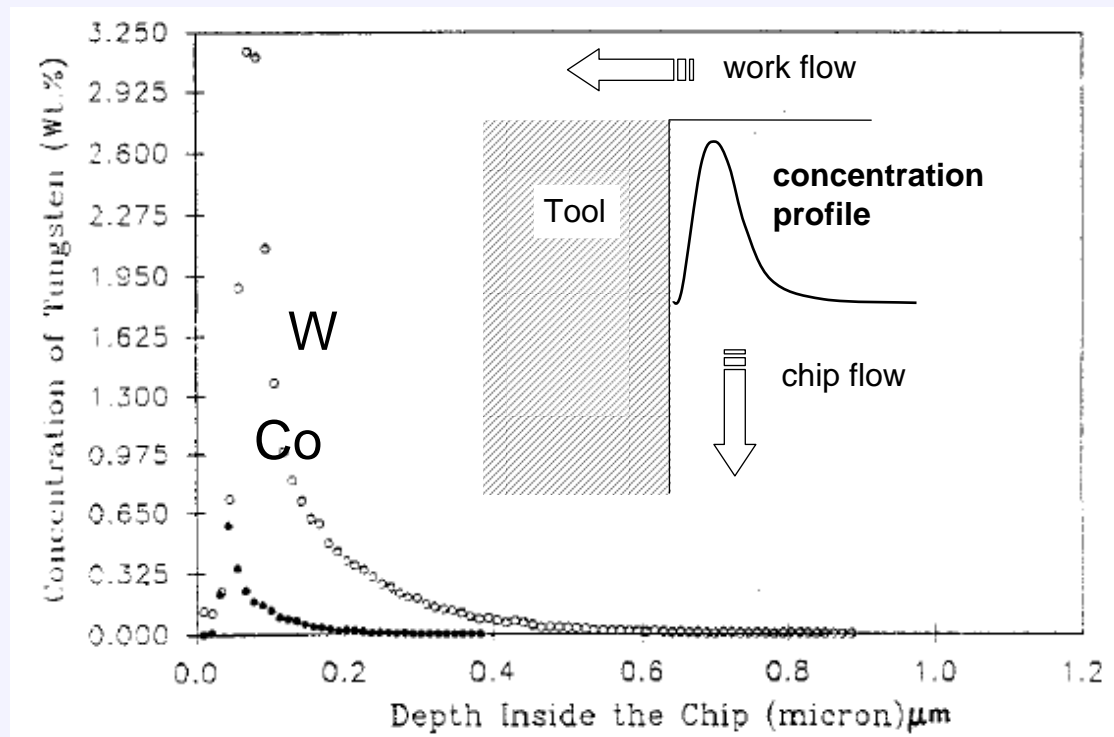
200x



# Verification of Tool Wear Mechanisms

Subramanian, Ingle, & Kay, *Surface and Coatings Technology*,  
61:293-299 (1993)

Secondary Ion Mass Spectroscopy



## Carbide Tools with a Ferrous Material



# Dissolution + Subsequent Diffusion

- Interactions within the chip's bulk

$$\frac{\partial X_i}{\partial t} = \text{div}(D_i \text{grad} X_i) - \text{grad} X_i \cdot \mathbf{v}^* - \frac{F_s}{c}$$

$$\frac{\partial X_V}{\partial t} = \text{div}(D_V \text{grad} X_V) - \text{grad} X_V \cdot \mathbf{v}^* - \frac{F_s}{c} + \frac{F_{V,psz}}{c}$$

$$\frac{\partial X_s}{\partial t} = -\text{grad} X_s \cdot \mathbf{v}^* + \frac{F_s}{c}$$

where  $\frac{F_s}{c} = k_f \left( X_i X_V - \frac{X_{i,eq} X_{V,eq}}{X_{s,eq}} X_s \right)$

and  $\frac{F_{V,psz}}{c} = k_V (X_{V,eq} - X_V)$

Frank-Turnbull Mechanism

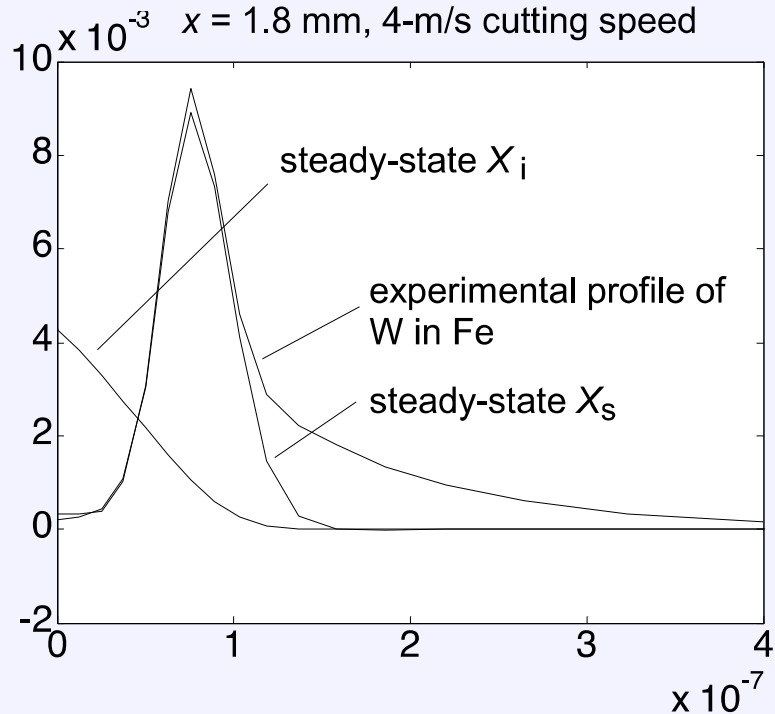
$X_{(i,V,s)}$  are the mole fractions of interstitials, vacancies, and substitutionals

$F_s/c$  : the rate of production of substitutional impurities via the Frank-Turnbull reaction

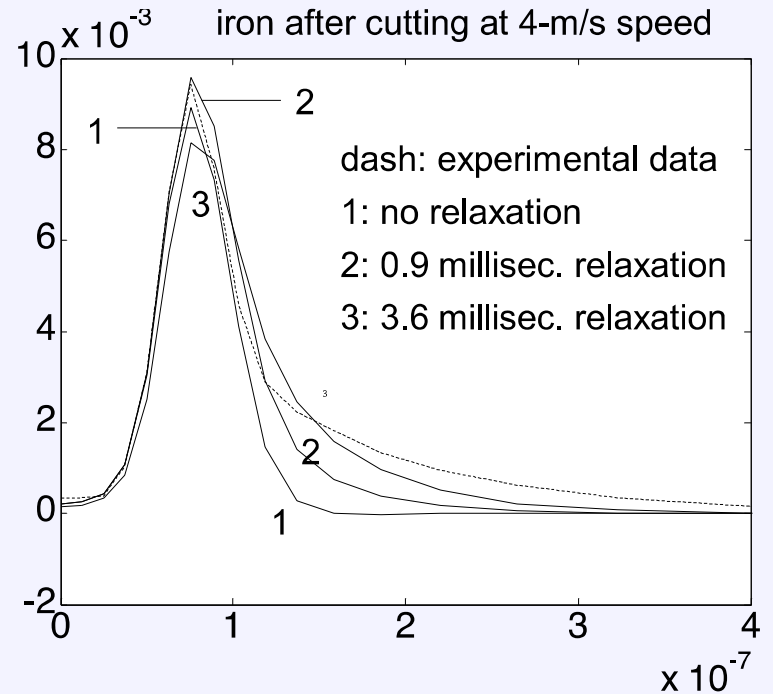


# Sectioned View, Steady State

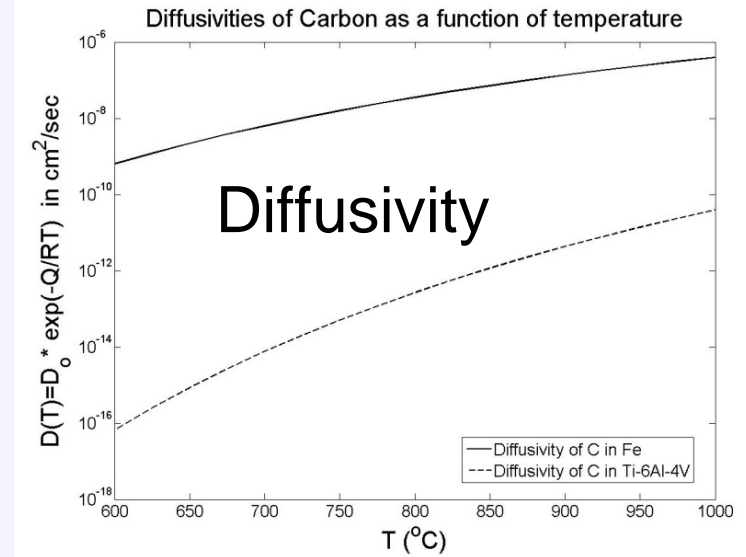
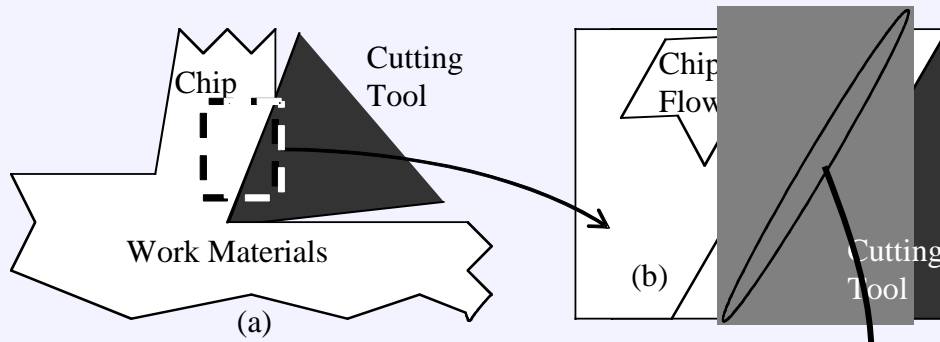
Comparison of W profiles in iron at  $x = 1.8$  mm, 4-m/s cutting speed



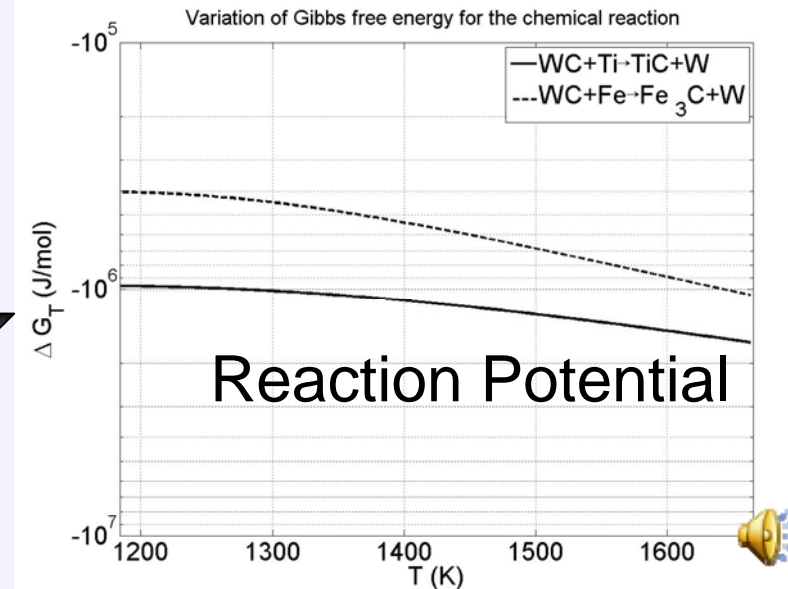
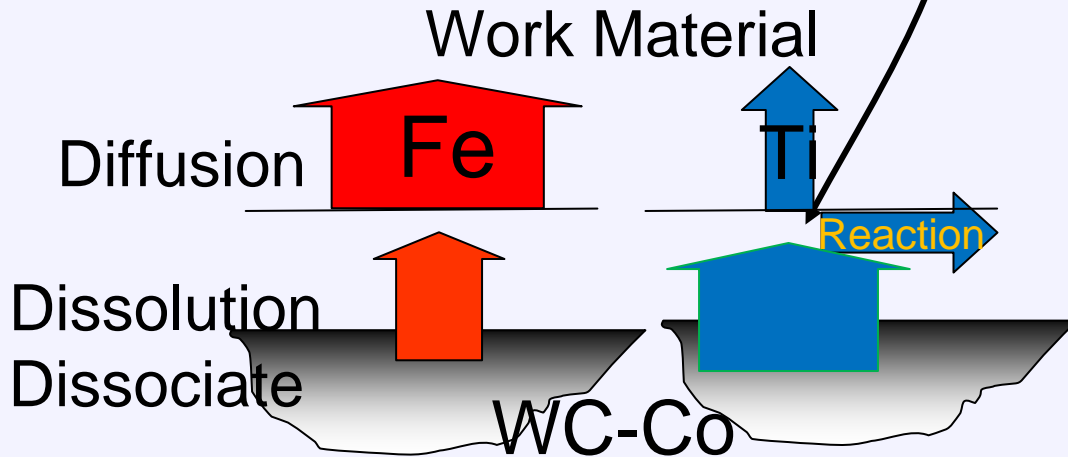
$X_s$ -relaxation profiles of tungsten in iron after cutting at 4-m/s speed



# Difference in Wear Mechanisms



## Traffic Jam Analogy



Dissolution controls in cutting steels  
Diffusion controls in cutting titanium



# Tool Wear During Turning of Ti-6Al-4V using PCD and Carbide Cutting Tools

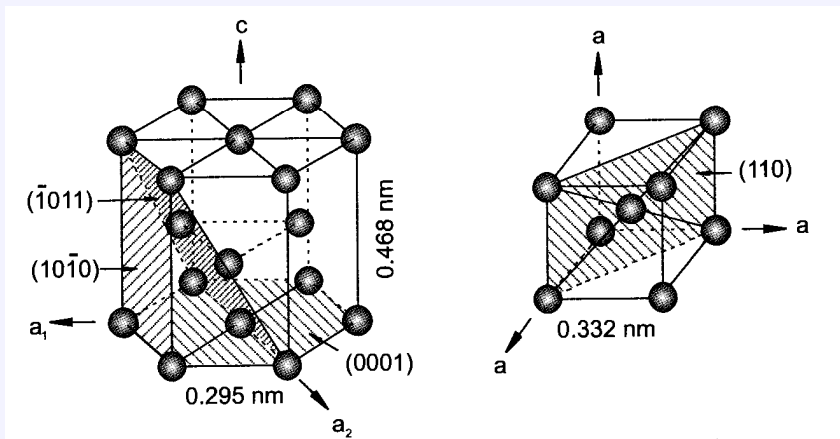
**ARMY - ARDEC**

David Schrock and Patrick Kwon  
Center for Advanced Cutting Tool Technology  
Michigan State University



# Ti-6Al-4V

- Two phase metal
  - HCP ( $\alpha$ - phase)
  - BCC ( $\beta$ -phase)
- Useful for Aerospace applications demanding high temperature strength to weight ratio and corrosion resistance
- Difficult to machine material
  - Low thermal conductivity
  - High reactivity
  - High strength at high temperature
  - Adhesion
- Current recommendations
  - Low cutting speed (<61m/min)
  - Flood cooling
  - Straight carbide cutting tools



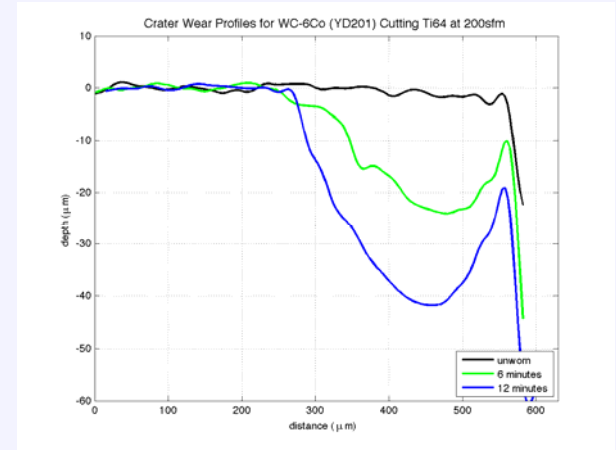
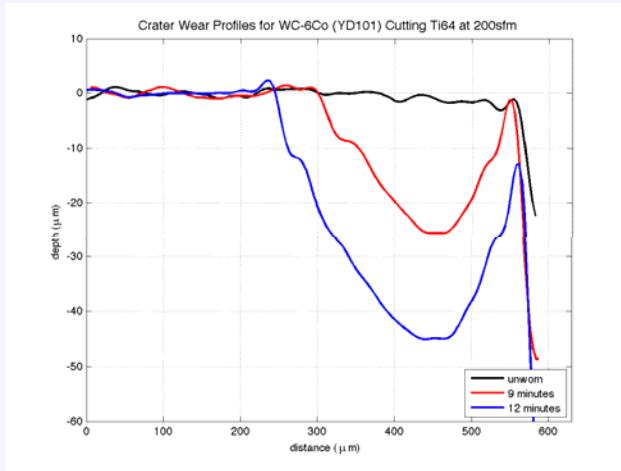
# Experimental Procedure



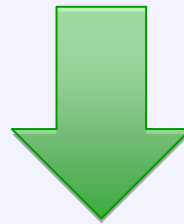
- Ti-6Al-4V work material turned on a YAMA SEIKI GA-30 lathe
- Cutting Tools
  - 2 grades of Carbide CNMA-432
    - YD101 (1 $\mu$ m ave. grain size)
    - YD201 (2 $\mu$ m ave. grain size)
  - PCD (Compax 1200P from Diamond Innovation) CNMA-432
    - with average grain size of 1.5  $\mu$  m with 92% volume.
    - 0 degree and 10 degree rake faces used
- Cutting Conditions
  - 3 Cutting speeds (61m/min, 92m/min, 121m/min)
  - Feed - .025mm/rev



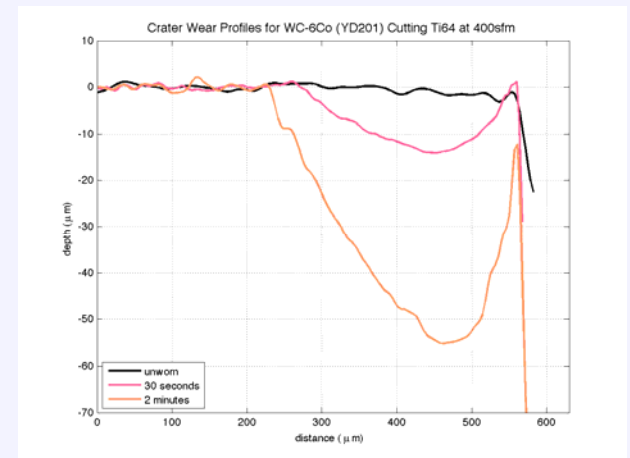
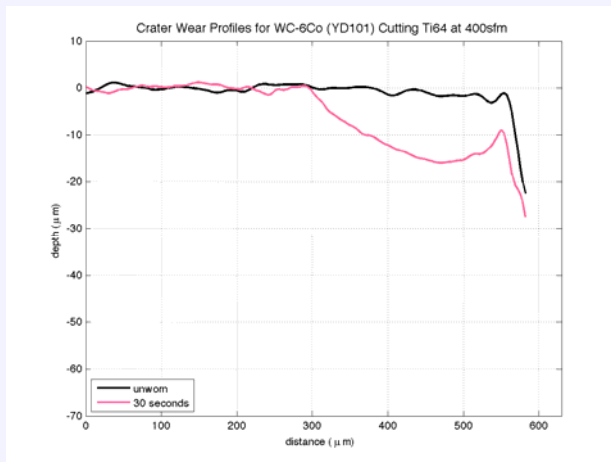
# Crater Wear Profiles



200sfm



400sfm



YD101

YD201

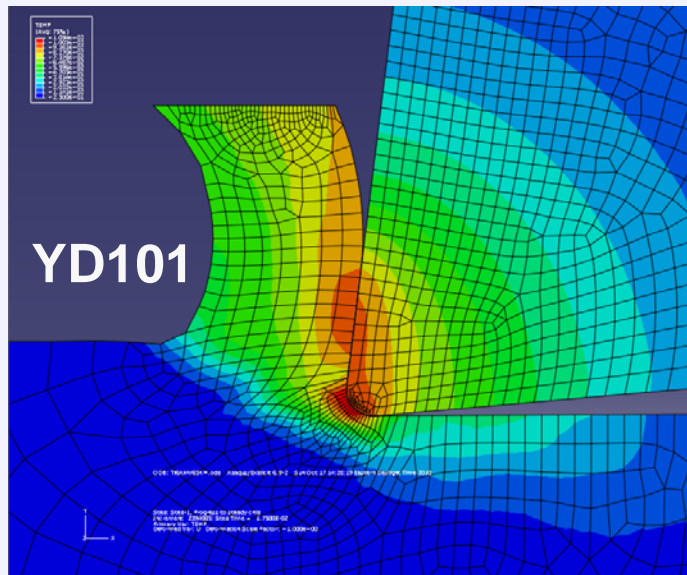
Slightly more crater wear on YD101 (smaller grains)



# FE Simulation at $v= 200\text{ft}/\text{min}$

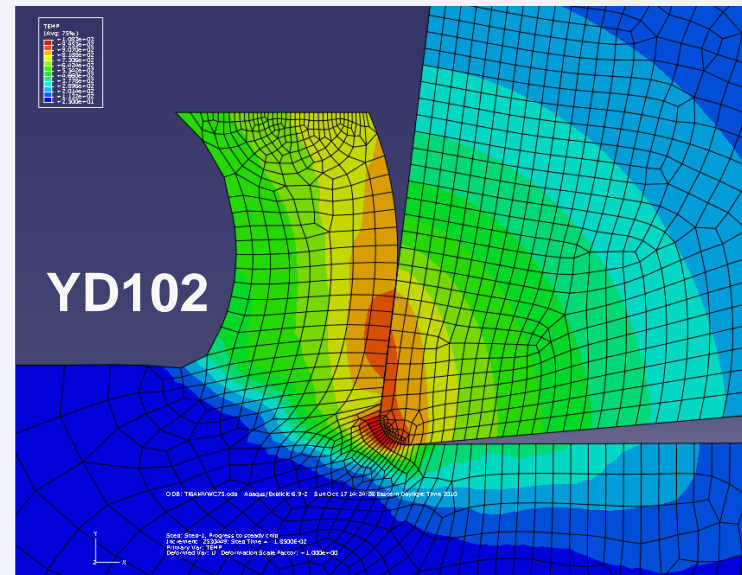
Work Material - Johnson-Cook model in literature

Tool Material - Thermally non-rigid but mechanically rigid



$$\kappa = 65\text{kW}/\text{m}$$

$$(T_{\text{max}} = 1095^\circ \text{ C})$$



$$\kappa = 75\text{kW}/\text{m} (T_{\text{max}} = 1085^\circ \text{ C})$$

The difference in the thermal conductivity ( $\kappa$ ).

At 200sfm, the temperature difference of  $10^\circ$ .

At 400sfm, the difference of  $15^\circ$ .



# Evidence of Phase-Dependent Tool Wear

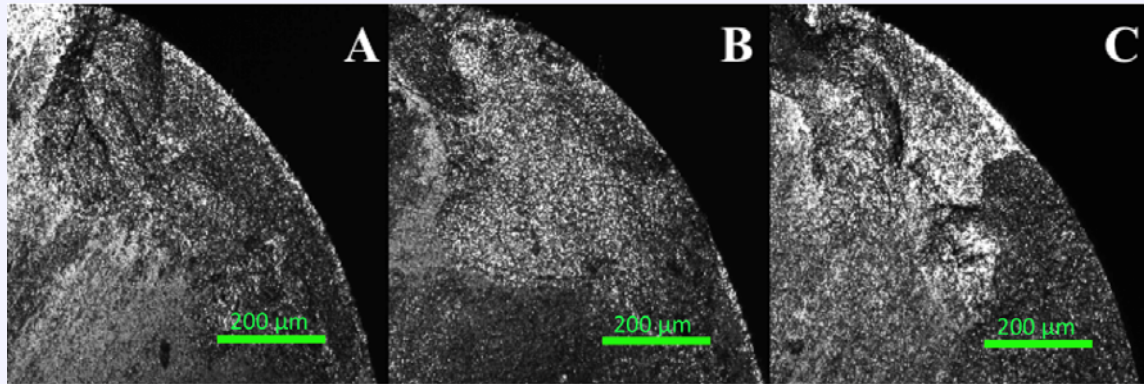


Figure: Rake face of PCD tools after cutting at 61m/min. Note the rough, scalloped surface

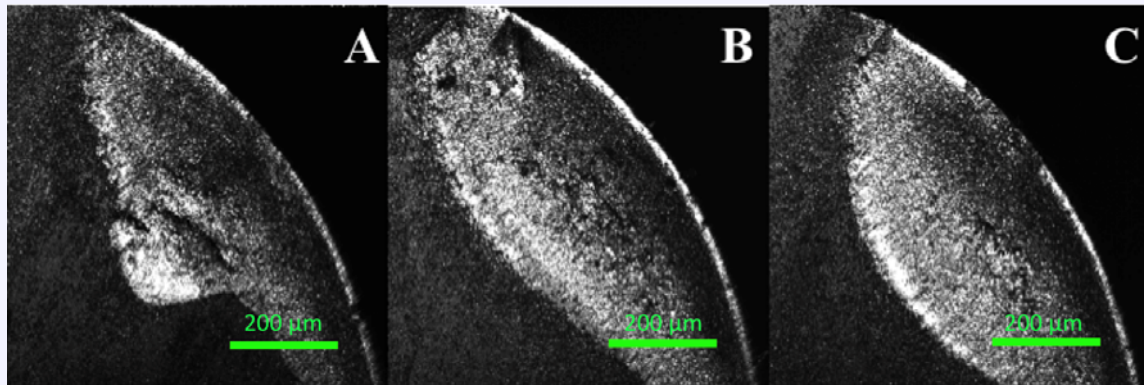


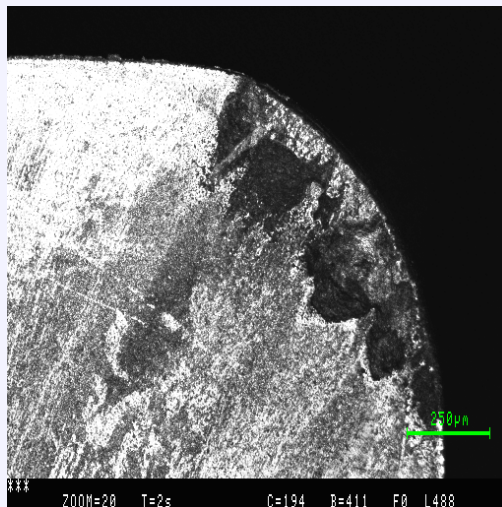
Figure: Rake face of PCD tools after cutting at 121m/min. Note the smooth craters



# PCD versus Carbide Tool Wear

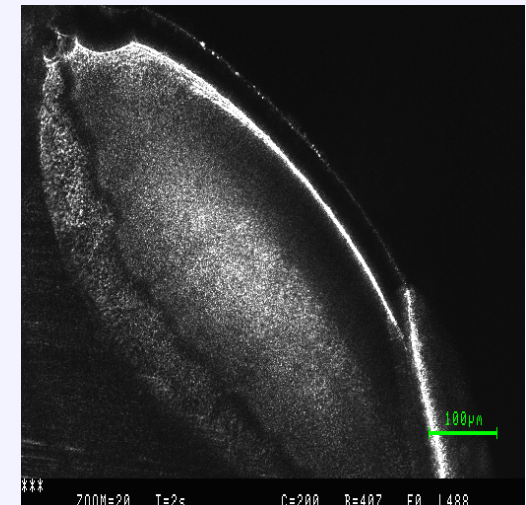
## PCD

- Phase change dependent tool wear previously discussed explains differences between wear at high and low cutting speeds



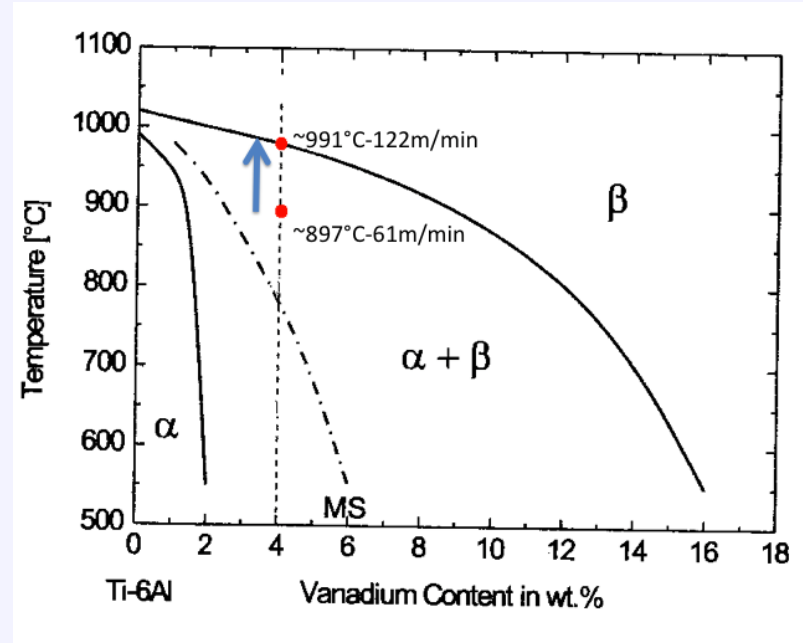
## Carbide

- FEM on the carbide tools predicts cutting temperature over 1000C for the carbide tools at 61m/min
  - Characteristic smooth craters for all cutting speeds



# Temperature from FEM

- FEM show temperatures for machining with PCD at 61m/min of 897C
  - From phase diagram, mostly alpha phase
- At high cutting speed, temperature approaches 1000C
  - Transformation to beta phase



Phase diagram for Ti-6Al-V system

Table 1: Temperature Estimation from FE Simulation

Cutting speed	PCD tools	WC-6Co tools
61m/min	897°C	1095°C
91m/min	942°C	1156°C
122m/min	991°C	1198°C





# Impact on Tool Wear

## Low Cutting Speed

- Chip is mainly  $\alpha$ -phase (HCP) or  $\alpha + \beta$  phase
  - Less favorable plastic deformation properties
    - Relative sliding at the tool work interface
    - Periodic separation of adhered material by fracture of tool, creating scalloped wear pattern
  - Much less self diffusivity
    - Fewer vacancies, slow dissolution wear

## High Cutting Speed

- Chip has transformed to  $\beta$  phase (BCC)
  - **Self-diffusivity 5 orders of magnitude higher for  $\beta$  at 1000C than for alpha at 500C**
    - Promotes generation vacancy dislocations which can accept interstitial carbon atoms (dissolution wear)
  - Improved plastic deformability
    - allows chip seizure, increasing dissolution wear
    - Separation of work material from tool occurs inside of chip
      - Prevents scalloped wear pattern



# Ongoing/Future Work

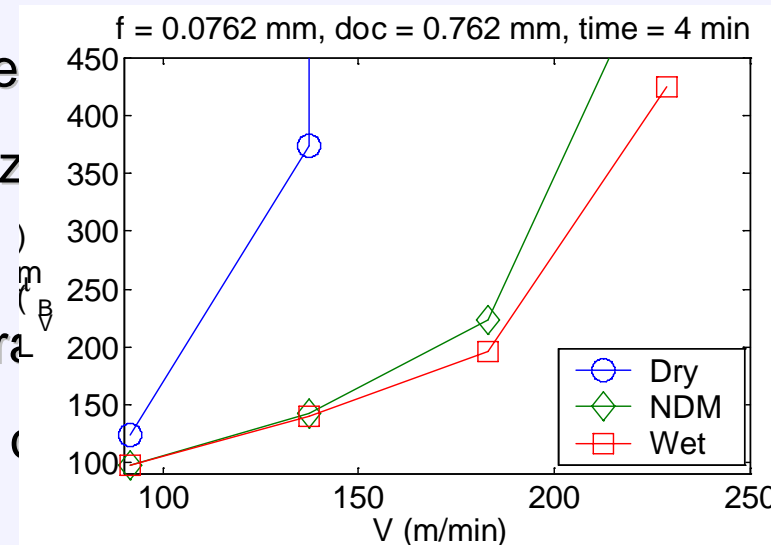
- SEM and optical microscopy to compare phases present in deformed chip to that of the unreformed work material
- Development of 3-d FEM simulation to more accurately predict temperature within tool material during cutting
- Determine investigate the kinetics of the phase change



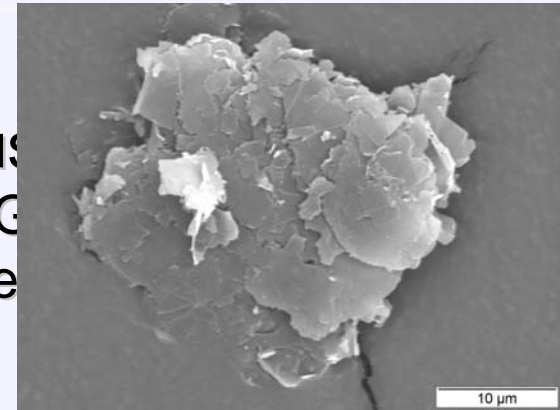
# Minimum Quantity Lubrication

- MQL Parameters which significantly influence on the effectiveness of MQL machining

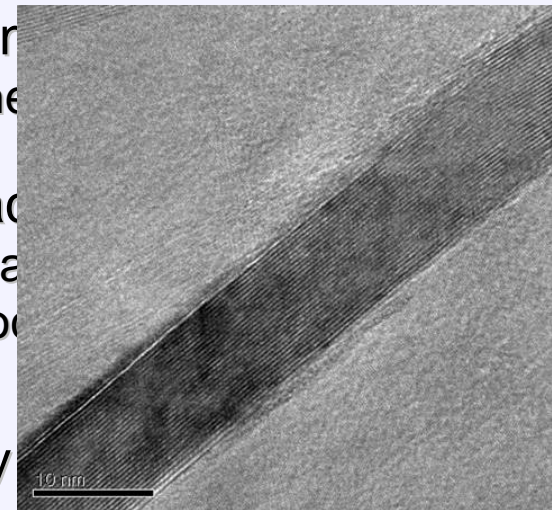
- Droplet size: oil mist size & health issue
- Droplet distribution: wetting area & nozzle distance
- Other parameters: Air pressure & flow rate
- Wetting angle: lubrication performance & coatings (?)
- Improvement of MQL lubricants



# x-GNP modified MQL oil



SUS  
(xG  
ide



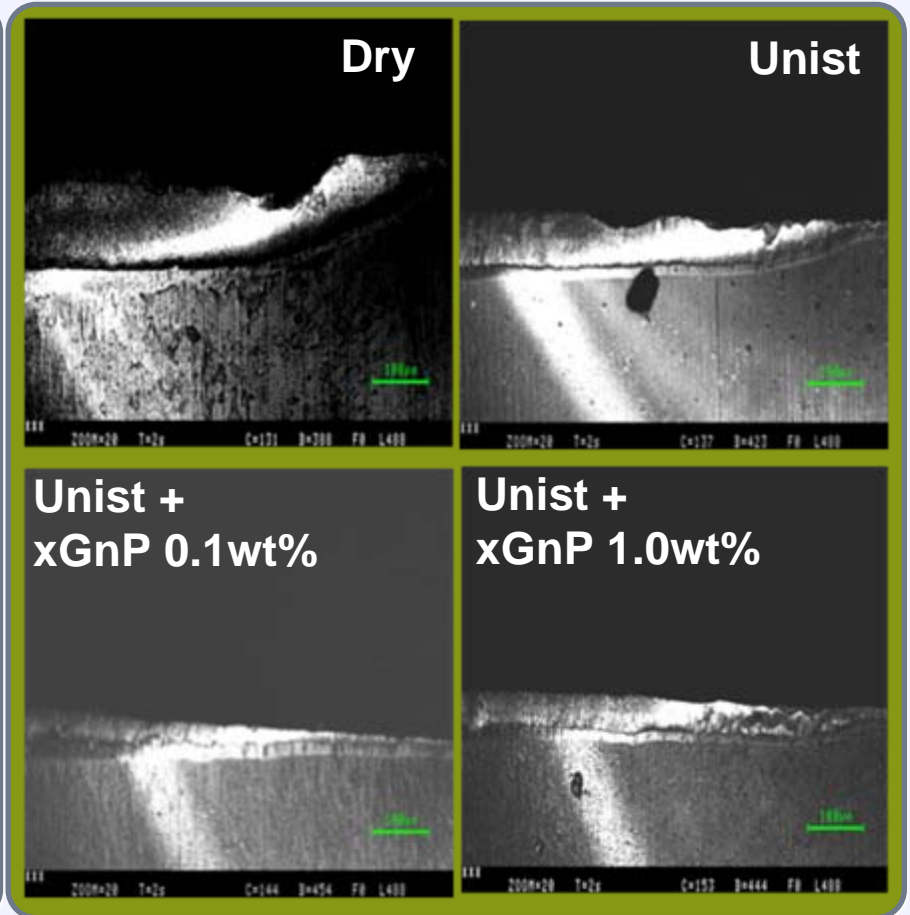
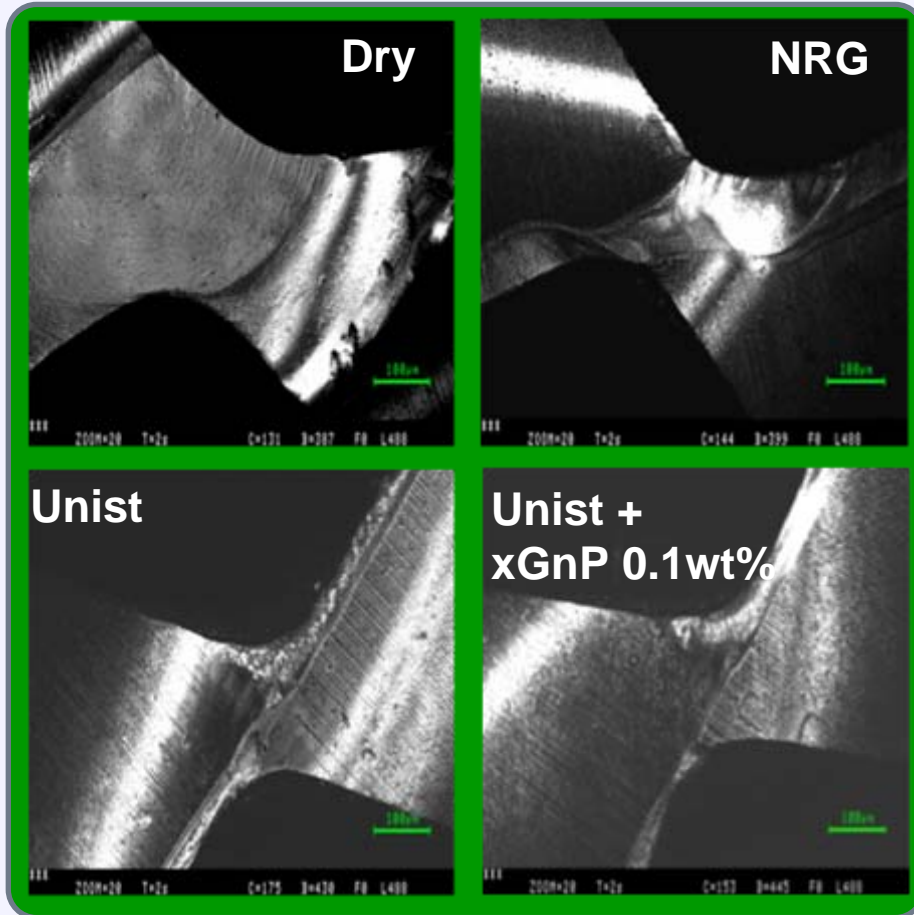
sion  
nthe  
trac  
sm  
e lo  
by



# Comparative Test

Central wear (8th layer) at 3500 RPM

Flank wear (8th layer) at 4500 RPM

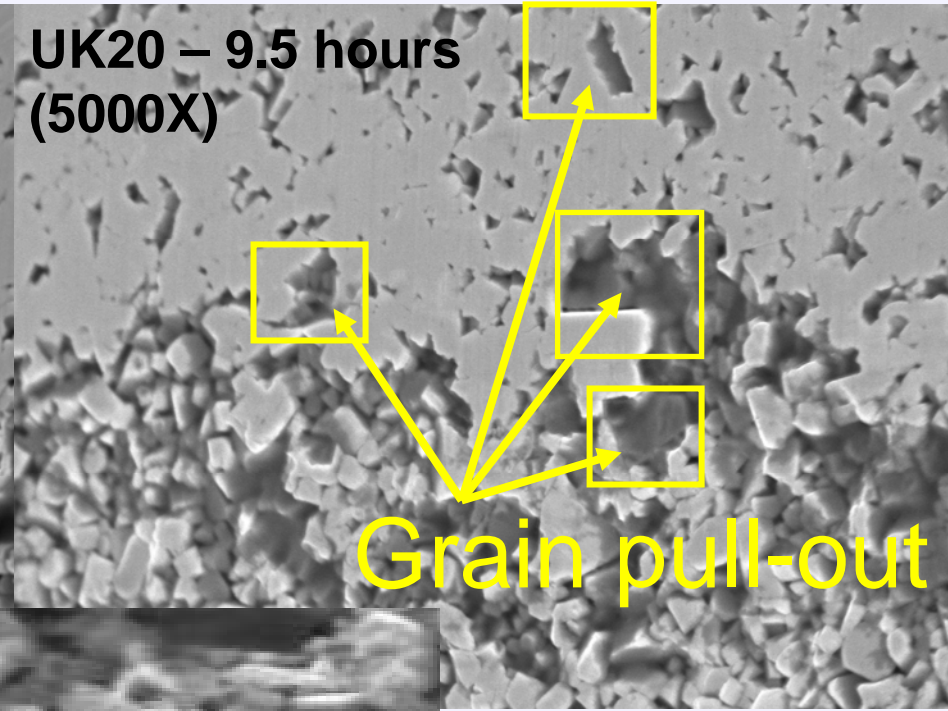
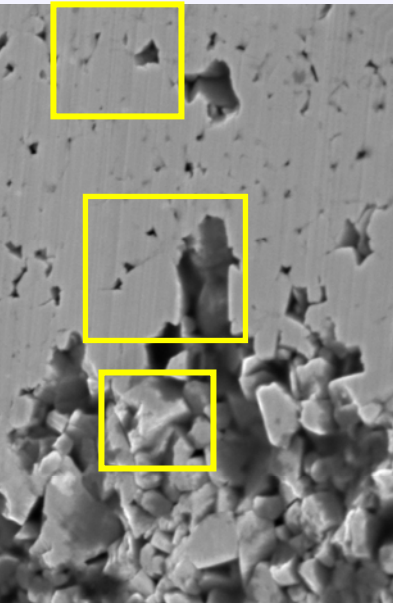
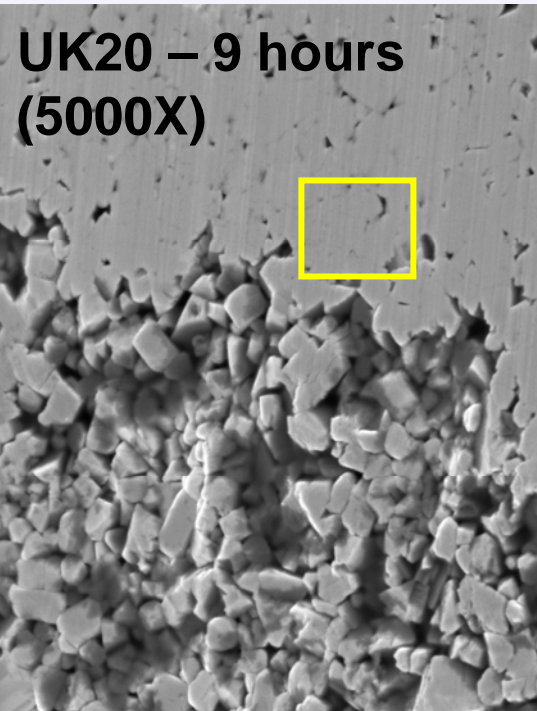


# Machining Soft Materials: Commercially Pure Aluminum

Xin Wang and P. Kwon  
Department of Mechanical Engineering  
Michigan State University  
East Lansing, MI

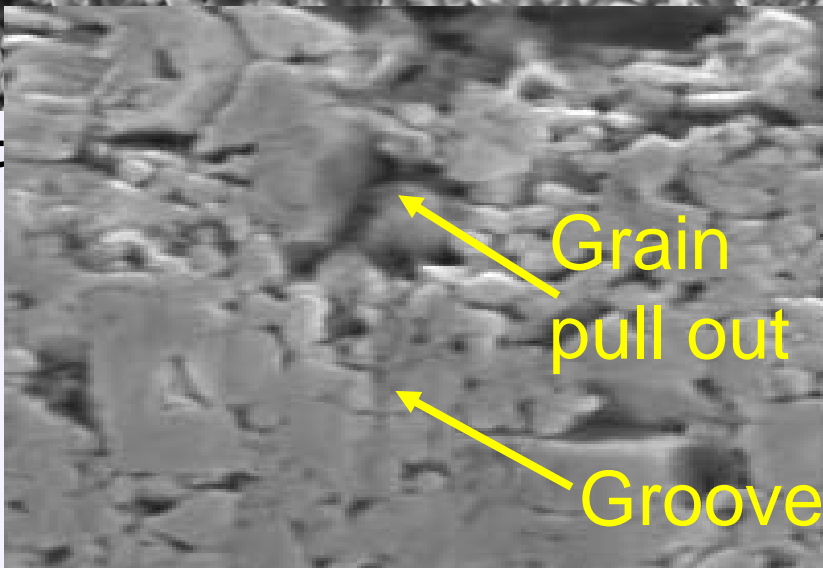


# Evidence of Carbide Grain Pull-out



Grain pull-out

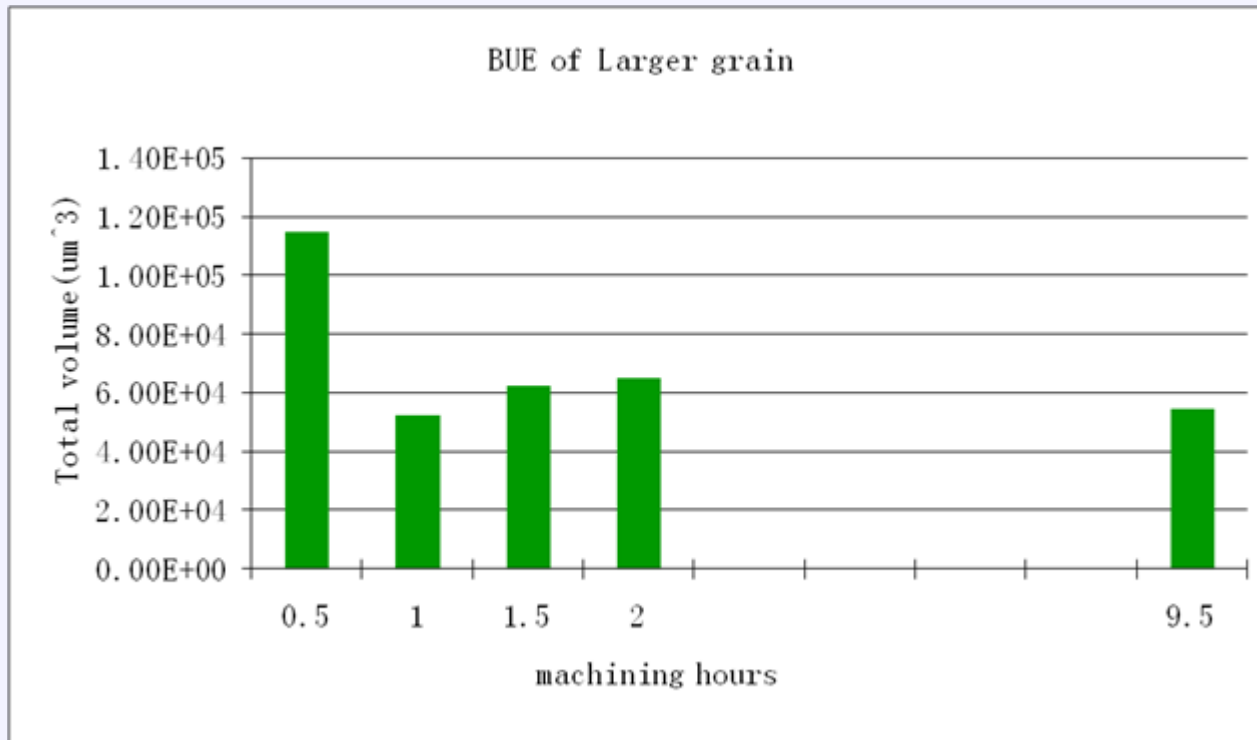
Grain pull-out after  
location on flank



at same



# BUE evolution

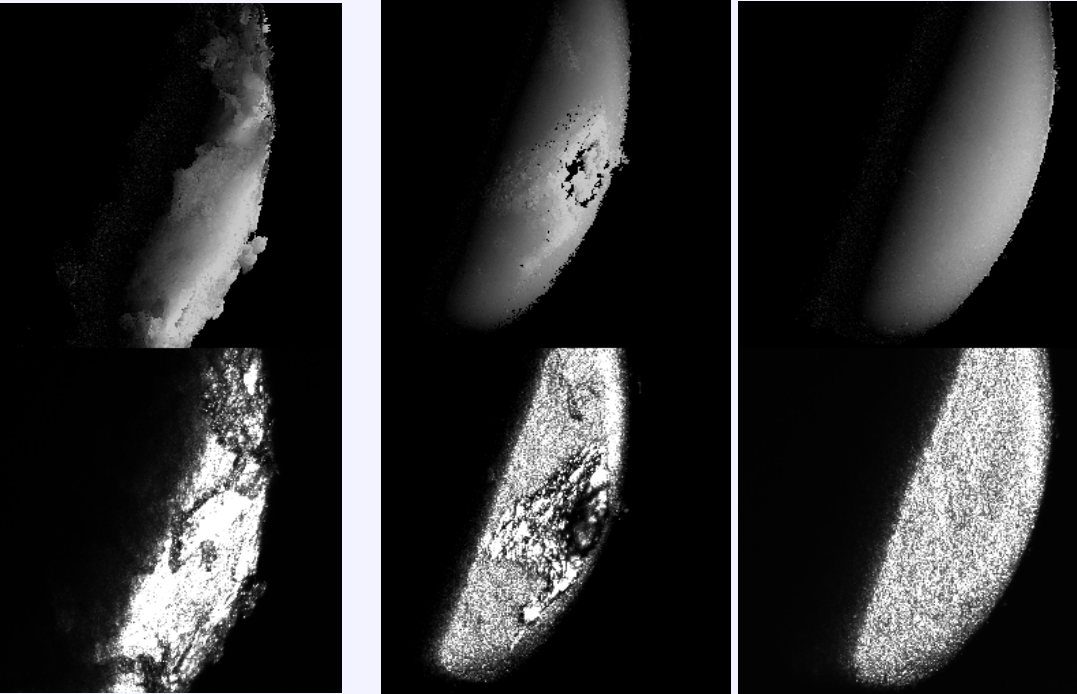


Evolution of volume of built up edge.





## 2 types of BUE



Element (at %)	Initial BUE	Thin layer
Al	77.65	68.48
C	19.54	21.92
O	2.63	9.41
Si	0.18	0.19
W	0	0

Before etching      etching for 2 hour & for 10 hours with 1% NaOH

- Carbon comes from the carbon contamination in SEM measurement.
- High concentration of oxygen was detected in the thin layer [6,7]. It indicates metal oxide exist in thin layer.



# Drilling CFRP/Ti Stack

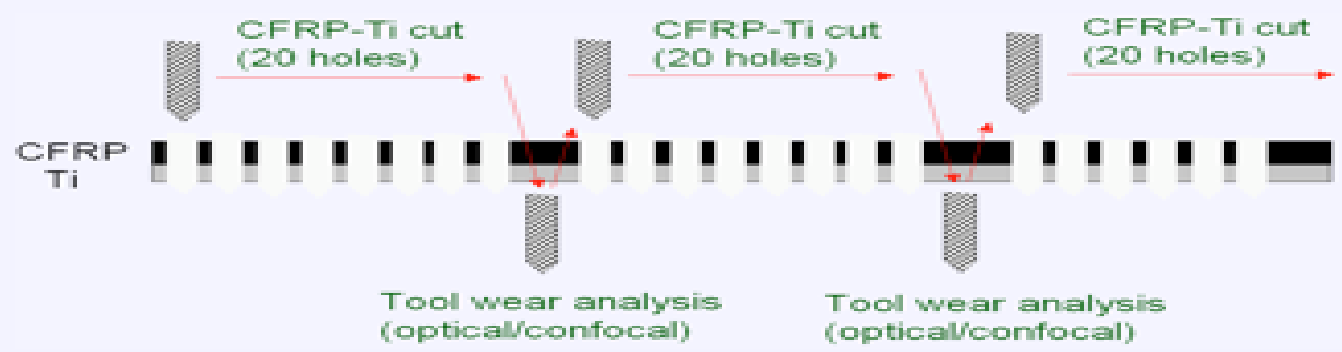
K. Park & X. Wang

Department of Mechanical  
Engineering



# Drilling Composite/Metal Stacks

- Drilling Experiments at WSU
  - CNC (HAAS Mini-Mill)
  - Carbide, PCD & BAM
  - Mist machining
- Post Analysis by MSU & WSU
  - Flank/Outer edge/Crater wear after every 20 holes (SEM, confocal microscope)

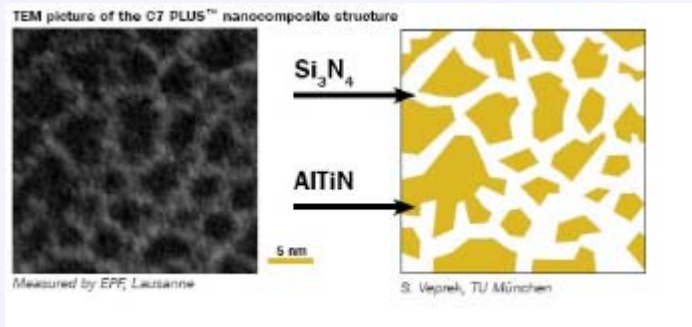


<b>Cutting tools (3 types)</b>	WC (10% Co micro-grain)	BAM coating (WC) (10% Co micro-grain)	PCD (Bimodal grade)
<b>Cutting speed</b>	CFRP 2000 rpm; Ti 400 rpm (WC) - 300 rpm (PCD)		
<b>Constant parameters:</b>	Drilling feed: 0.0762 mm/rev (CFRP) and 0.0508 mm/rev (Ti) Coolant: Water-soluble cutting fluid, Mist coolant flow rate at 16 mL/min.		



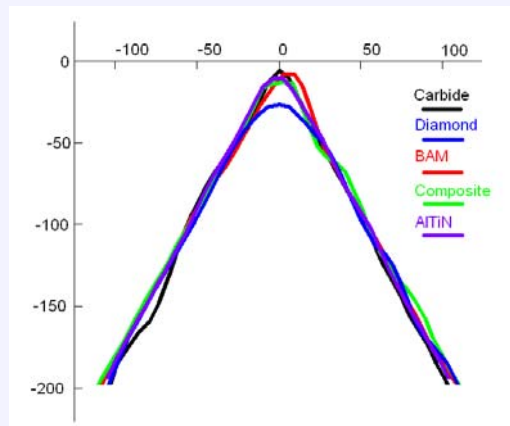
# Tool coatings

1. CVD Diamond coating – Boeing
2. BAM coating – Fraunhofer
3. Nanocomposite coating – Unimerco's C7 Plus



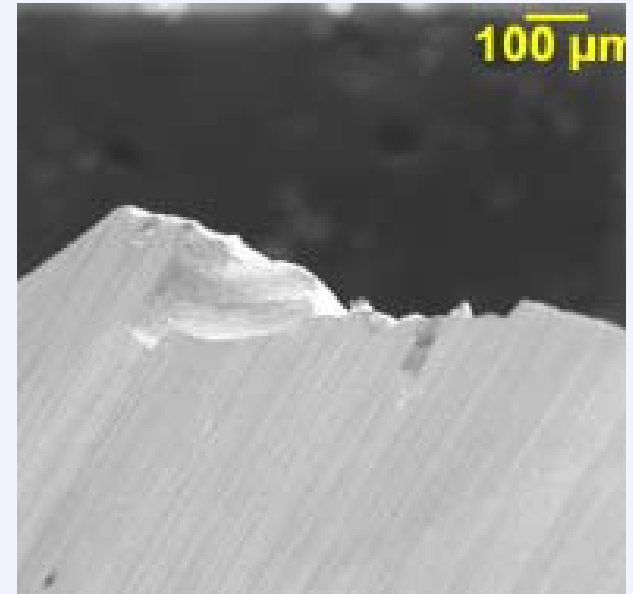
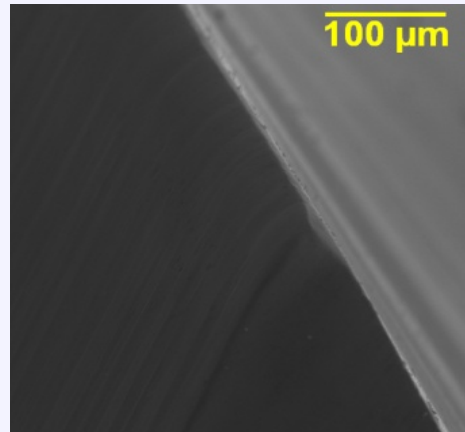
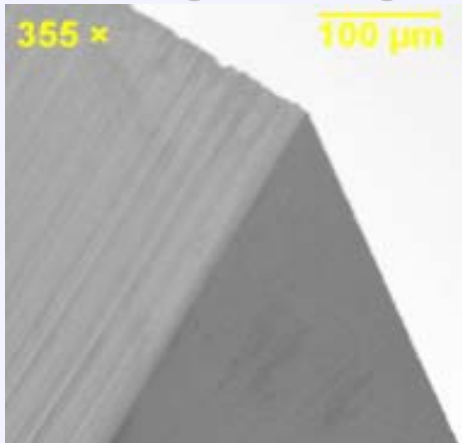
4. AlTiN coating – Unimerco (from Europe)

Coating	Cutting edge angle (°)	Coating thickness
Uncoated	59.2	/
BAM	58.7	3.5 μm
Diamond	61.2	12.5 μm
Composite	57.0	3 μm
AlTiN	60.2	3 μm

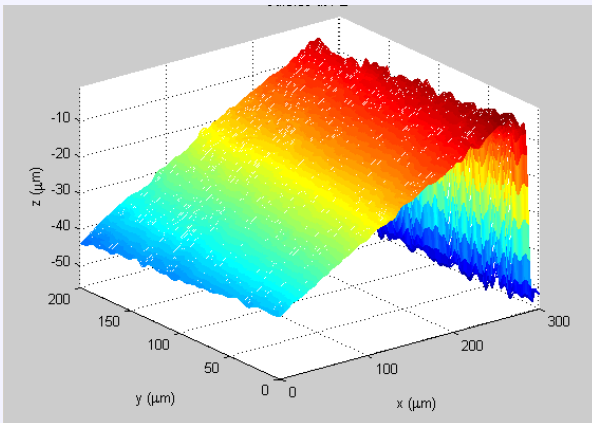


# Observation

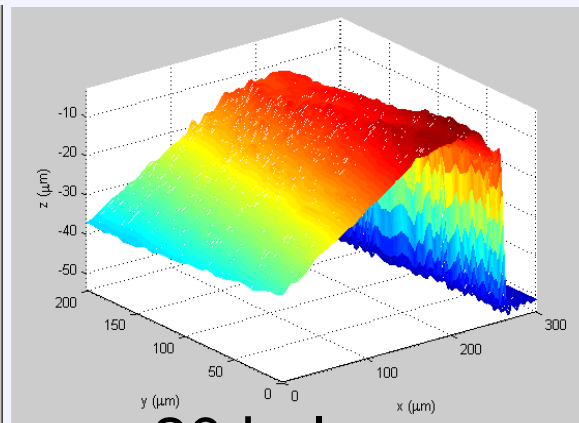
- Tool wear in CFRP drilling was blunting the edge.



- Tool wear in TI drilling was Chipping.



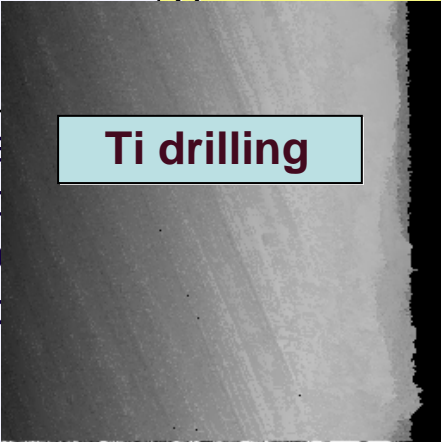
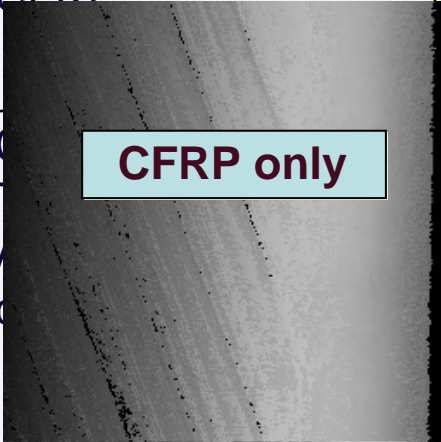
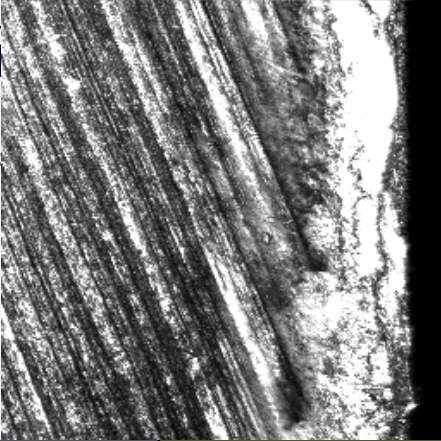
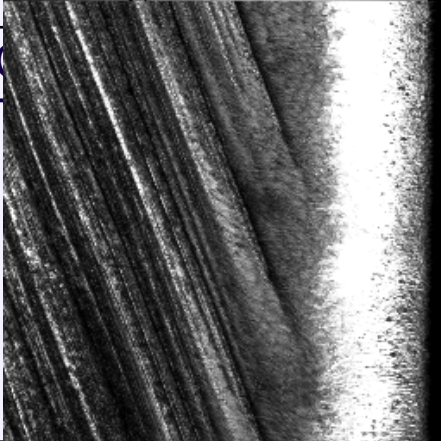
New



20 holes



# Wear Mechanism - Stack

	CFRP	Ti	CFRP	Ti
Carbide	Abrasive wear to carbon fibers through 2-body abrasion process	 <p><b>Ti drilling</b></p>	 <p><b>CFRP only</b></p>	Ti adhesion → WC grains pulled out as built-up-Ti removed
PCD	Minimal tool wear due to high hardness of			Ti adhesion + Major chipping areas get larger due to additional chipping



# Edge blunting wear in CFRP drilling

- Our hypothesis is
  - In metal machining, stagnation zone protect the cutting edge. In CFRP machining, there is **no stagnation zone** to protect the cutting edge

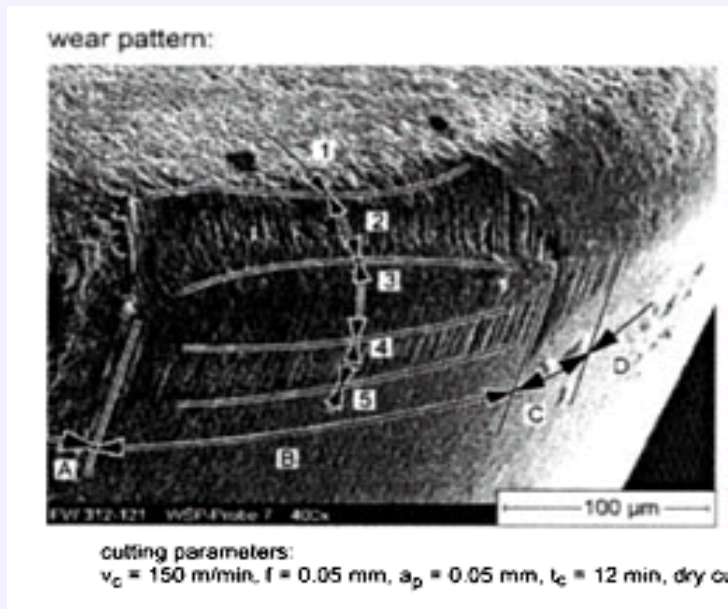


Figure 1. Wear pattern of a PCBN tool in hardened steel machining

Zone 2 (crater wear)

Zone 4 (flank wear)

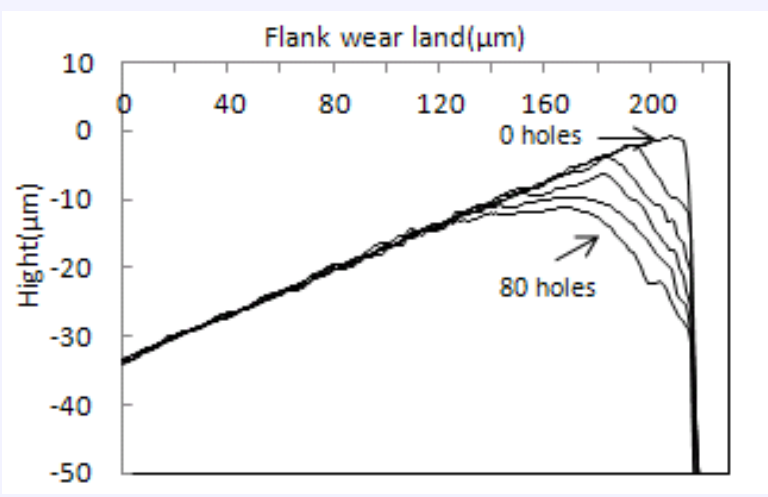
Zone 3 (cutting edge – no wear)

Cutting edge has no wear in metal machining.

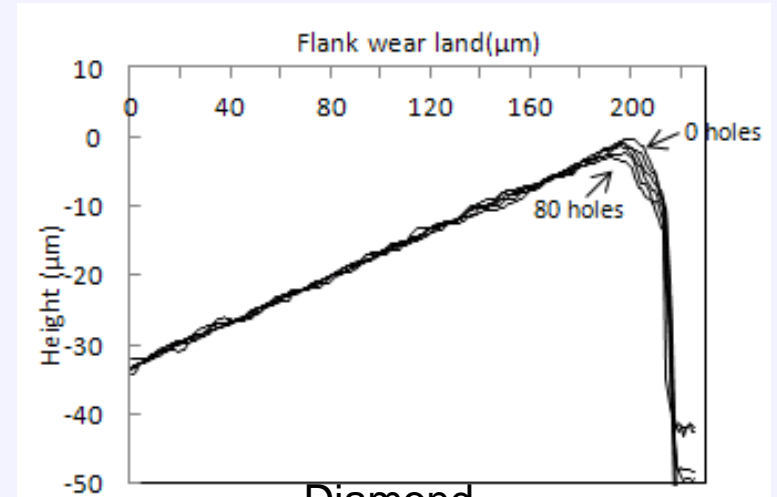
Because there is no relative sliding or very slow sliding of work material on the cutting edge of the tool.



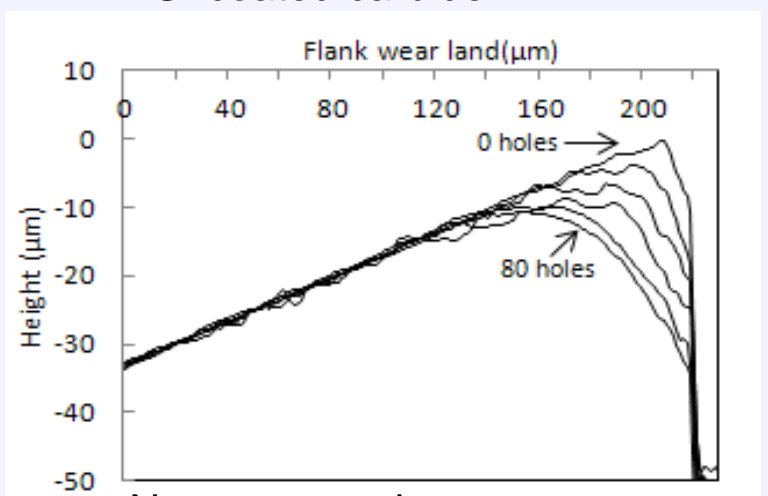
# Wear of coated drills (CFRP)



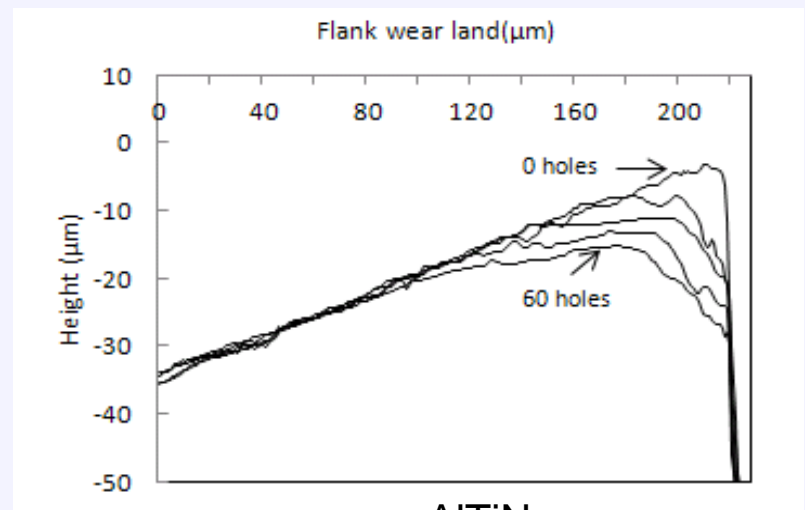
Uncoated carbide



Diamond



Nano-composite



AlTiN





# Wear mechanism in CFRP drilling

## ■ Abrasive wear or sliding wear?

**Table 2.** Abrasive wear rate and sliding wear rate of the coatings

	Hardness at 25° C (GPa)	Relative abrasive wear rate	Sliding wear rate (mm <sup>3</sup> /Nm)	Relative sliding wear rate
Uncoated carbide	26	1	1.39E-07	1
Diamond	70	0.007	1.22E-08	0.088
BAM	43	0.078	7.27E-07	5.230
AlTiN	40	0.113	3.98E-07	2.863

Wear volume (um <sup>2</sup> )	Total wear	Relative coatings wear rate
Uncoated	641	1
Diamond	71	0.111
BAM	1015	3.992
Composite	761	1.811
AlTiN	944	2.772

Abrasive wear rate of coating was predicted by the coating hardness data and abrasive wear equation.

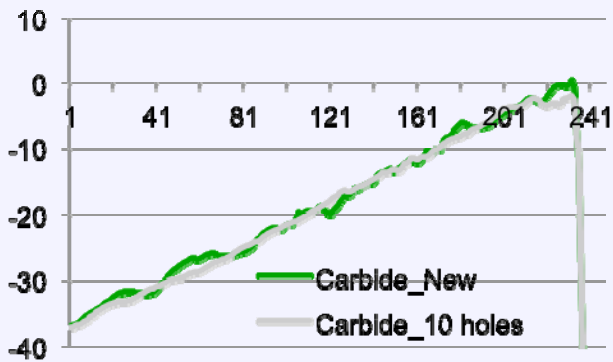
Sliding wear rate was acquired by a tribo-meter test experiment.

(Sliding wear is too complicated, and could not be predicted by material property. )

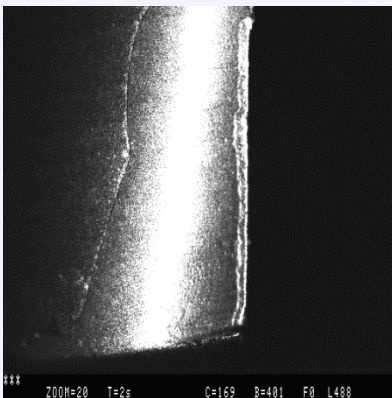


# Tool wear in Ti drilling

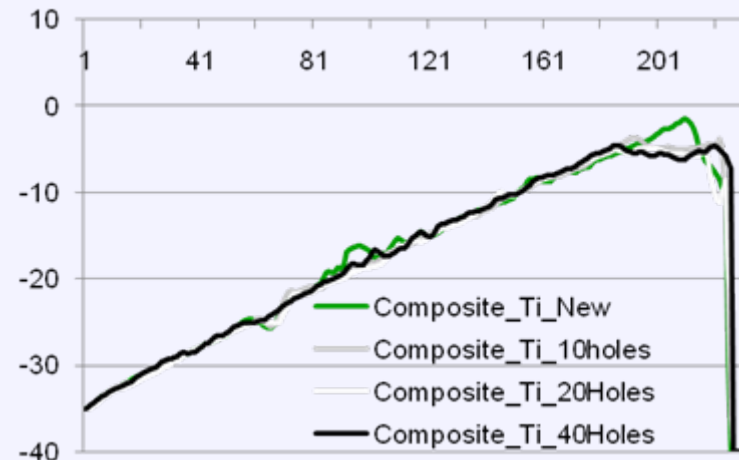
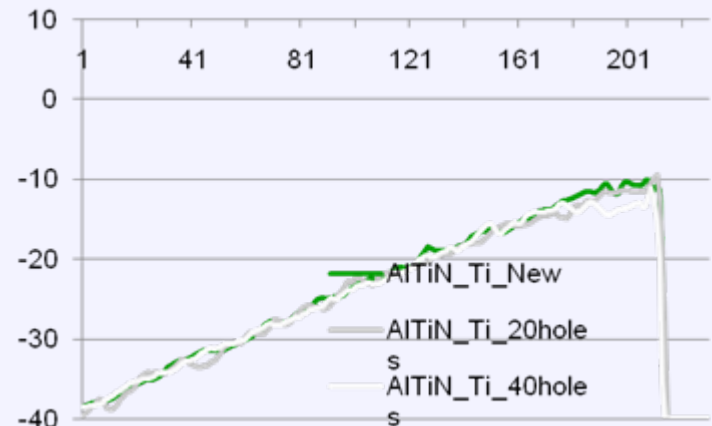
- Besides the edge chipping, the tool wear in Ti drilling is much smaller than in CFRP drilling.



Carbide: Edge chipping at 20 holes

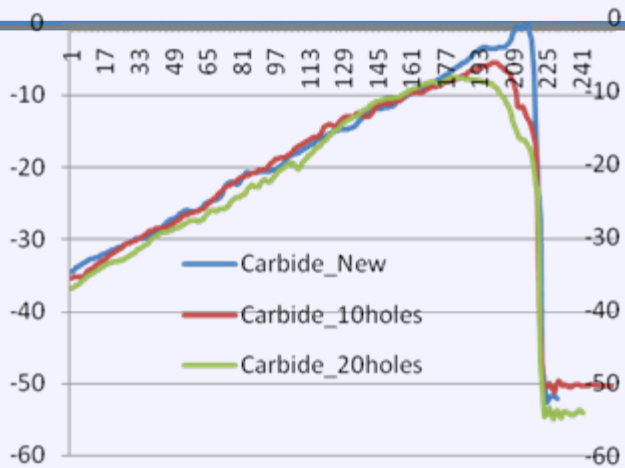


Diamond: Coating flake off at 10 holes

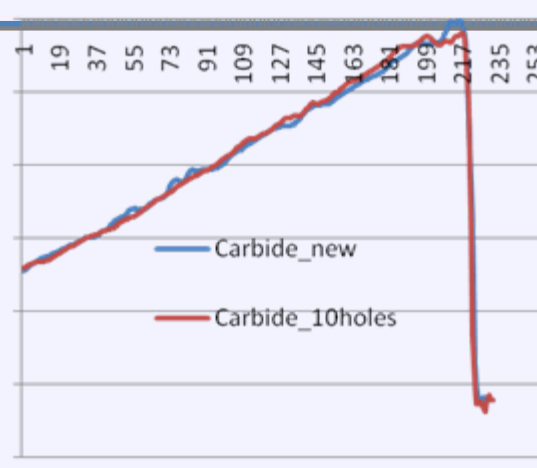


# Uncoated Carbide Tools

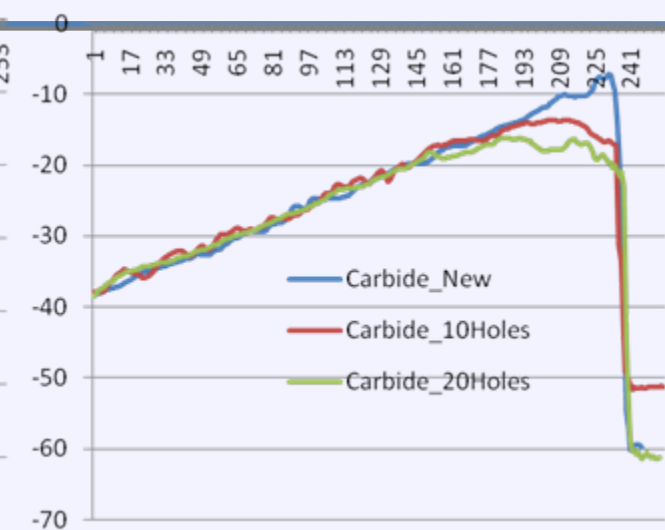
Wear on CFRP only +  
Wear on Ti only =  
Wear on Stack



CFRP only



Ti only

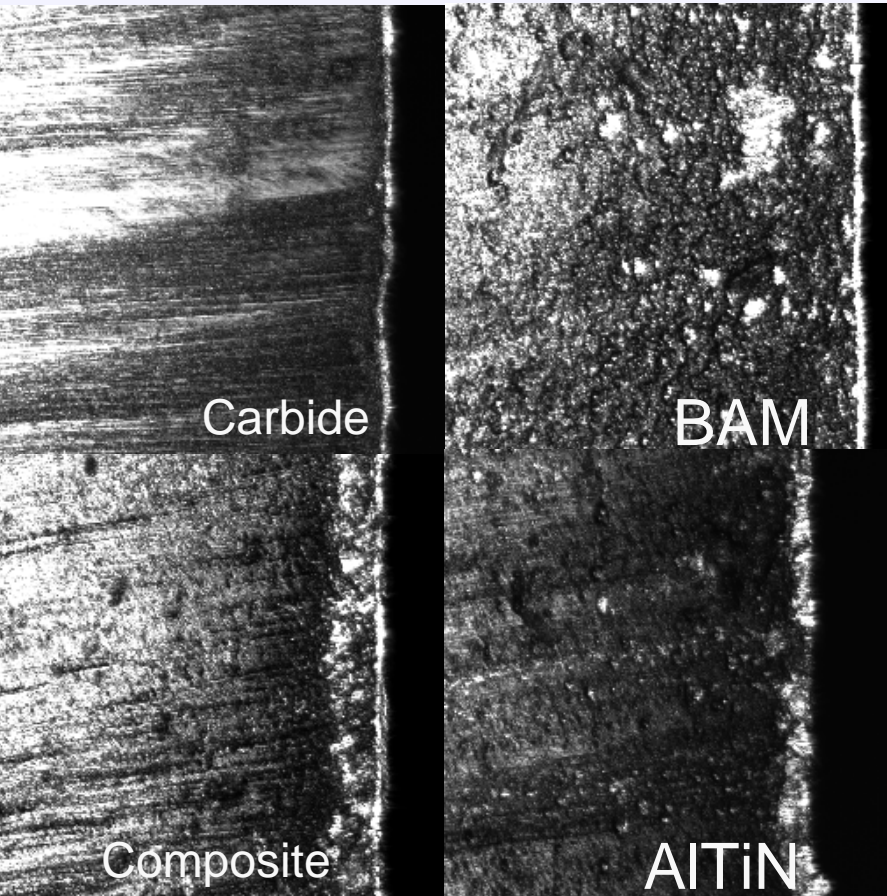


Stack

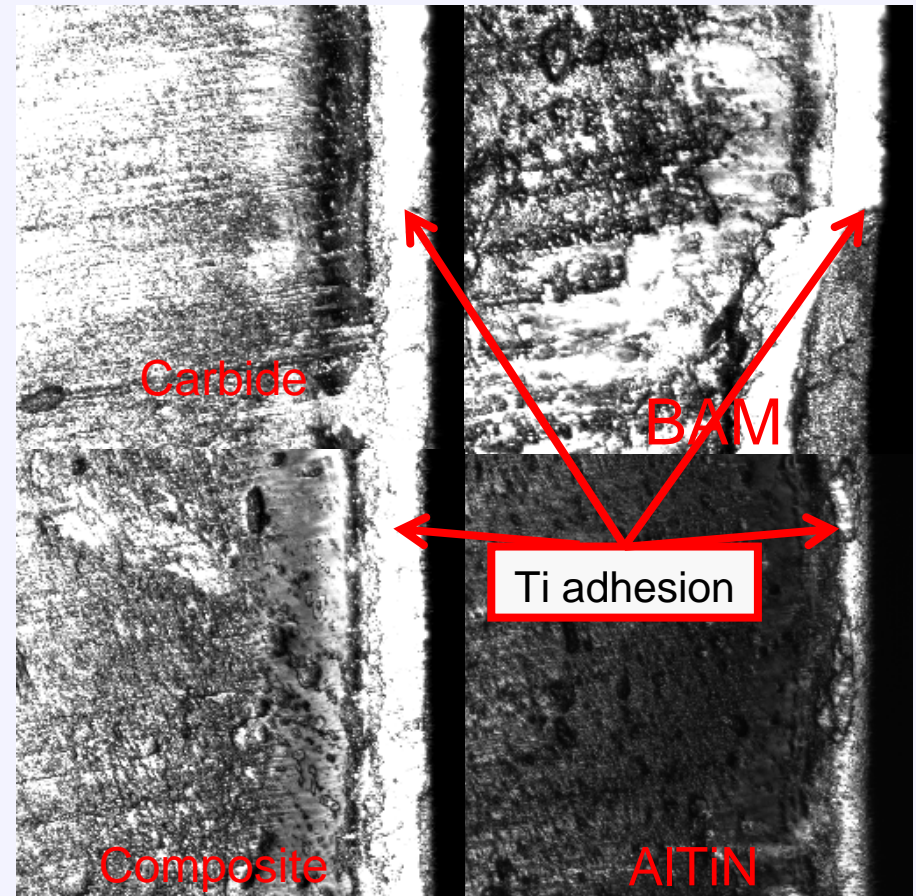


# Comparison of Ti and Stack drilling

Ti drilling 20 holes



Stack drilling 20 holes



More titanium adhesion in stack drilling than Ti drilling.  
It may due to the edge rounding in stack drilling  
-> more stagnation material at the cutting edge



# Conclusion

- The edge blunting (dulling, rounding) wear in CFRP machining is due to lack of a work material stagnation zone in front of the cutting edge, which would normally prevent the edge wear.
- The sliding wear rather than abrasive wear in CFRP machining.
  - Hard coating without good sliding wear resistance do not increase the tool life.



# Acknowledgement

- NSF for supporting I/UCRC on Advanced Cutting Tool Technology
- Boeing
- Los Alamos National Laboratory
- Fraunhofer CCL
- Valenite Inc.
- ARMY-ARDEC
- (New Tech Ceramics, Sandvik, Unimerco, GM & UNIST)

